

1 **The origin(s) and geodynamic significance of Archaean ultramafic-mafic bodies**
2 **in the mainland Lewisian Gneiss Complex, North Atlantic Craton**

3 George L. Guice^{a,b,*}; Iain McDonald^b; Hannah S. R. Hughes^{c,d}; John M. MacDonald^e;
4 John W. Faithfull^f

5

6 ^a National Museum of Natural History, Smithsonian Institution, 10th & Constitution Avenue, Washington,
7 D.C. 20560. USA.

8 ^b School of Earth and Ocean Sciences, Cardiff University, Main Building, Park Place, Cardiff. CF10 3AT. UK.

9 ^c Camborne School of Mines, College of Engineering, Mathematics & Physical Sciences, University of Exeter,
10 Penryn Campus, Penryn, Cornwall, TR10 9FE, UK.

11 ^d School of Geosciences, University of the Witwatersrand, Private Bag 3, Wits 2050, Johannesburg South
12 Africa.

13 ^e School of Geographical and Earth Sciences, Gregory Building, University of Glasgow, Glasgow, G12 8QQ

14 ^f Hunterian Museum, University of Glasgow, University Avenue, Glasgow, G12 8QQ

15

16 *corresponding author: GuiceG@si.edu

17

18

19 **Keywords:** Archaean geodynamics; Archean; cratonisation; North Atlantic Craton; Lewisian; PGE;
20 granulite; layered intrusion; mantle

21 **ABSTRACT**

22 The geodynamic regime(s) that predominated during the Archaean remains controversial, with the
23 plethora of competing models largely informed by felsic lithologies. Ultramafic-mafic rocks displaying
24 distinctive geochemical signatures are formed in a range of Phanerozoic geotectonic environments.
25 These rocks have high melting points, making them potentially useful tools for investigating Archaean
26 geodynamic processes in highly metamorphosed regions. We present field mapping, petrography,
27 traditional bulk-rock geochemistry, and platinum-group element geochemistry for 12 ultramafic-mafic
28 bodies in the Lewisian Gneiss Complex (LGC), which is a highly metamorphosed fragment of the North
29 Atlantic Craton in northwest Scotland. Our data indicate that most of these occurrences are layered
30 intrusions emplaced into the tonalite-trondhjemite-granodiorite (TTG)-dominated crust prior to
31 polyphase metamorphism, representing a significant re-evaluation of the LGC's magmatic evolution.
32 Of the others, two remain ambiguous, but one (Loch an Daimh Mor) has some geochemical affinity
33 with abyssal/orogenic peridotites and may represent a fragment of Archaean mantle, although further
34 investigation is required. The ultramafic-mafic bodies in the LGC thus represent more than one type
35 of event/process. Compared with the TTG host rocks, these lithologies may preserve evidence of
36 protolith origin(s), with potential to illuminate tectonic setting(s) and geodynamic regimes of the early
37 Earth.

38

39

40

41

42

43 INTRODUCTION

44 Plate tectonics is the unifying theory of modern geological knowledge, providing a framework for the
45 interpretation of Earth's Phanerozoic geology. However, the nature and timing of its onset remains a
46 matter of considerable debate (Arndt, 2013; Cawood et al., 2018; Kamber, 2015), leading to the
47 proposal of a plethora of competing geodynamic models to explain the Archaean Earth (e.g., Bédard,
48 2018; Bédard et al., 2013; Brown and Johnson, 2018; Johnson et al., 2019, 2017; Kamber, 2015; Van
49 Kranendonk et al., 2004). Recently, in an attempt to pinpoint a date for the onset of plate tectonics,
50 authors have assessed the temporal variation of a variety of geological and geochemical proxies. Such
51 proxies include: (i) the presence/absence of passive margins and paired metamorphic belts (Brown
52 and Johnson, 2018; Cawood et al., 2018); (ii) various element ratios recorded by the bulk-rock
53 geochemical composition of granitoid (Halla, 2018; Johnson et al., 2019) and/or mafic rocks (Condie,
54 2018; Dhuime et al., 2015; Moyen and Laurent, 2018; Smithies et al., 2018); and (iii) the apparent
55 thermal gradients (T/P) of peak metamorphism (Brown and Johnson, 2018). This global approach has
56 been successful in identifying a significant evolution in Earth's behaviour between ~3.3 Ga and ~2.5
57 Ga, with such evolution perhaps pertaining to the onset of Earth's current geodynamic regime (see
58 Cawood et al. 2018). However, this approach does not provide material evidence of the specific
59 geodynamic processes that operated throughout the Archaean Eon. Part of the challenge, when
60 studying rocks of this age, is the likelihood for primary signatures to be overprinted by metamorphism
61 and associated processes, such as partial melting and metasomatism.

62 On the modern Earth, ultramafic-mafic rocks are both formed and preserved in a variety of
63 geodynamic environments, displaying distinctive geological associations and geochemical signatures.
64 For example, the residual mantle portion of an ophiolite exhibits significant trace element depletion
65 (Godard et al., 2008; Paulick et al., 2006) relative to mantle derived melts that may crystallise as
66 komatiites or the ultramafic-mafic portions of a layered intrusion (Furnes et al., 2012). Moreover,
67 when compared to felsic lithologies, the constituent minerals of ultramafic rocks have high melting

68 temperatures, making them relatively resilient to the subsequent effects of high-temperature
69 metamorphism and associated partial melting (Bowen, 1956). Therefore, if the effects of alteration
70 and associated metasomatism, which are often cryptic, can be constrained (Guice, 2019; Guice et al.,
71 2019, 2018b), ultramafic-mafic rocks have the potential to establish the physical manifestations of
72 Archaean geodynamic processes. Specifically, confident identification of residual mantle rocks
73 associated with age equivalent intrusions and submarine lavas (as part of an ophiolite that displays
74 structural and lithological relationships comparable to Phanerozoic examples) would represent
75 extremely strong evidence in favour of plate tectonics having operated (Bédard et al., 2013; Kamber,
76 2015; Rollinson, 2007). Presently, suggested Archaean ophiolite occurrences remain highly contested,
77 with the proposed examples often not withstanding detailed examination (Guice et al., 2019; Szilas et
78 al., 2018, 2015).

79 The ultramafic-mafic complexes of the mainland Lewisian Gneiss Complex (LGC) – a classic and
80 intensely studied portion of Archaean crust located in NW Scotland – have been interpreted as
81 representing mafic magmatism in settings that reflect different Archaean geodynamic regimes. Such
82 interpretations include: (i) remnants of an early, possibly oceanic, mafic-ultramafic crust (Sills, 1981);
83 (ii) fragments of one or more layered intrusions emplaced into existing crust (Bowes et al., 1964; Guice
84 et al., 2018a); (iii) accreted oceanic crust (Park and Tarney, 1987); or (iv) the sagducted remnants of
85 one or more greenstone belt(s) (Johnson et al., 2016). In a recent study, which utilised detailed field
86 mapping, petrography and spinel mineral chemistry, Guice et al. (2018a) interpreted the Ben Strome
87 Complex as representing a layered intrusion emplaced into the tonalite-trondhjemite-granodiorite
88 (TTG)-dominated crust prior to granulite-facies metamorphism at ~2.7 Ga. This interpretation of the
89 Ben Strome Complex, which represents the largest (7 km²) and best exposed ultramafic-mafic complex
90 in the mainland LGC, is counter to the bulk of previous literature, which, based on the seemingly
91 dispersed nature of the ultramafic-mafic rocks (e.g., Park et al., 2002) and an apparent (but contested;
92 Guice et al., 2018a; Johnson et al., 2016) cross-cutting relationship at Geodh' nan Sgadan (Rollinson
93 and Windley, 1980; Fig. 1), assumes that these lithologies pre-date the TTG protoliths. If this

94 interpretation withstands further interrogation and is extended to other ultramafic-mafic complexes
95 in the region, it requires a significant re-evaluation of the magmatic evolution of the LGC. Moreover,
96 multiple studies have suggested that the ultramafic-mafic rocks of the mainland LGC may reflect more
97 than one origin (Guice et al., 2018a; Rollinson and Gravestock, 2012), potentially recording multiple
98 phases of temporally and/or petrogenetically distinct phases of Archaean ultramafic-mafic
99 magmatism, including the potential incorporation of Archaean mantle fragments.

100 In this paper, we present field mapping and observations, petrography, major and trace element bulk-
101 rock geochemistry, and, for the first time, platinum-group-element (PGE) bulk-rock geochemistry for
102 12 ultramafic-mafic complexes in the mainland LGC. The spatial distribution of the ultramafic-mafic
103 complexes is detailed in Figure 1. Using the presented data, we aim to:

- 104 (i) Examine the validity of the layered intrusion hypothesis (“Ben Strome model”) for
105 other ultramafic-mafic complexes in the mainland LGC;
- 106 (ii) If/where this hypothesis fails, assess the possibility that fragments of Archaean
107 mantle may be preserved within this portion of the North Atlantic Craton.

108 **REGIONAL GEOLOGY**

109 The mainland LGC crops out as a 125 x 20 km coastal strip located in northwest Scotland, west of the
110 Moine Thrust (Peach et al., 1907; Sutton and Watson, 1951; Wheeler et al., 2010). Partially covered
111 by Neoproterozoic to Ordovician sedimentary rocks, the mainland LGC is dominated by amphibolite-
112 to granulite-facies TTG gneiss and has experienced a protracted and complex history of magmatism,
113 metamorphism and deformation (Peach et al., 1907; Wheeler et al., 2010). Volumetrically subordinate
114 ultramafic, mafic and metasedimentary rocks accompany the TTG gneiss, with all these lithologies
115 cross-cut by a suite of Palaeoproterozoic mafic dykes (the “Scourie Dykes”) and later pegmatitic sheets
116 in some areas (Park et al., 2002). Traditionally, the mainland LGC has been subdivided into a granulite-
117 facies Central Region and amphibolite-facies Northern and Southern Regions (Fig. 1). Relative to the
118 hornblende-bearing Northern and Southern Regions, the pyroxene-bearing Central Region is depleted

in Cs, Rb, U, Th, K and Ta (Sheraton et al., 1973), with the latter interpreted as representing deeper crustal levels than the former (Park and Tarney, 1987). More recently, geochronological-based studies, which utilise U-Pb dating of zircon in TTG gneiss, have shown that the mainland LGC records a wide range of protolith ages and metamorphic histories (Friend and Kinny, 2001; Kinny et al., 2005; Kinny and Friend, 1997; Love et al., 2010, 2004), with the mainland LGC therefore interpreted to represent up to six “terrane”. Although the precise number of terranes remains controversial (Park, 2005), the Laxford Shear Zone (see Fig. 1) is generally accepted as a significant crustal boundary (Goodenough et al., 2013, 2010).

Although many aspects of the magmatic and metamorphic evolution remains the topic of considerable discussion, it is generally accepted that the magmatic precursors to the TTG gneiss crystallised between 3.1 and 2.7 Ga (Friend and Kinny, 2001; Kinny et al., 2005; Love et al., 2010; MacDonald et al., 2015; Whitehouse and Kemp, 2010). A widespread granulite-facies tectonothermal event – known locally as the Badcallian – most likely occurred between 2.8 and 2.7 Ga, with peak *P-T* conditions estimated at 0.8-1.2 GPa and > 900°C (Andersen et al., 1997; Barnicoat, 1983; Barnicoat and O’Hara, 1978; Barooah and Bowes, 2009; Cartwright et al., 1985; Corfu, 1998; Corfu et al., 1994; Crowley et al., 2015; Evans and Lambert, 1974; Feisel et al., 2018). This event, which is characterised by a pervasive, shallow- to moderate-dipping gneissosity that displays open to isoclinal folds (Guice et al., 2018a; Park et al., 2002), likely led to partial melting of the TTG gneisses and some mafic lithologies (Johnson et al., 2013, 2012). The Badcallian was succeeded by a granulite- to amphibolite-facies tectonothermal event – known locally as the Inverian – between c. 2.5 and 2.4 Ga (Beach, 1974, 1973; Corfu et al., 1994; Whitehouse and Kemp, 2010). This event, which is poorly constrained due to subsequent reactivation, is defined as preceding the 2.42-2.38 Ga emplacement of the NW-SE-trending Scourie Dykes (Davies and Heaman, 2014; Heaman and Tarney, 1989). These steeply-dipping dykes can be up to 100 m wide, with the NW-SE trend likely controlled by pre-existing shear zones (Weaver and Tarney, 1981). Finally, a greenschist- to amphibolite-facies tectonothermal event(s) – known locally as the Laxfordian – occurred between c. 1.9 and 1.6 Ga, forming E-W-trending shear

zones that are typically tens of metres wide and characterised by a thinning of the Badcallian foliation, and, especially north of the Laxford shear zone, granite emplacement (Beach, 1974; Beach et al., 1974; Goodenough et al., 2013, 2010).

FIELD RELATIONSHIPS

With the exception of the Loch an Daimh Mor and Geodh' nan Sgadan Complexes, the studied ultramafic-mafic complexes (namely: Achiltibuie, Achmelvich, Ben Auskaird, Ben Strome, Drumbeg, Loch Eilean na Craoibhe Moire, North Scourie Bay and Scouriemore) share several characteristics. Exposed across areas up to 7 km², these complexes are composed of modally layered ultramafic and mafic rocks (Fig. 2). This layering is extremely striking in the ultramafic rocks (Fig. 3a-c), but, as a consequence of the greater susceptibility to metamorphism (i.e., partial melting), is more discrete in the mafic rocks (Fig. 3d). There is a consistent parallelism between the gneissose foliation in the surrounding TTG, layering in the ultramafic-mafic rocks, and all lithological contacts (Fig. 2), as described by previous studies (Bowes et al., 1964; Guice et al., 2018a; Johnson et al., 2016). The ultramafic portions comprise dominant metapyroxenite (metawebsterite and metaolivine-websterite) and rare metaperidotite (metalherzolite), while the mafic portions contain metagabbro, garnet-metagabbro, garnet-amphibolite and amphibolite in variable proportions. The contacts between the complexes and surrounding TTG gneiss are tectonic where observed, but actual exposures are remarkably scarce. Similarly, although many of the contacts between ultramafic and mafic units are also rare, those observed are gradational on a scale of tens of centimetres (Guice et al., 2018a).

Individual ultramafic units can be traced for hundreds of metres along strike and are mostly several metres to several tens of metres in apparent thickness (Fig. 2a-b). The metawebsterites within these ultramafic portions have distinctly grey weathered surfaces and generally show little-to-no internal layering, while the grey-brown metaolivine-websterites and brown metaperidotites exhibit prominent internal layering (Fig. 3a-c). The metaolivine-websterite and metaperidotite layers are generally negatively weathered relative to the pyroxenitic layers. Moreover, the ultramafic rocks in all of these

complexes consistently exhibit gradational and sharp contacts between individual layers; gradational variation in modal mineral abundances within individual layers; and truncation of layers on the centimetre-scale (Fig. 3a-c). The mafic portions of these complexes comprise garnet-metagabbro, metagabbro, garnet-amphibolite and amphibolite in varying proportions. In places, the mafic rocks show centimetre- to metre-scale layering that is more discrete than in the ultramafic rocks, with individual layers defined by the proportions of garnet, pyroxene and plagioclase (Fig. 3d). Garnet, which commonly occurs on the centimetre-scale and often exhibits retrogressive plagioclase and/or amphibole rims, may form large clots up to 1 m in diameter. Millimetre- to centimetre-scale horizons containing high proportions of oxide minerals (dominantly magnetite and ilmenite) occur rarely (e.g., at Ben Strome; NC 25716/36120).

While sharing the salient features outlined above, these complexes also exhibit some variation in structural architecture (Fig. 2). For example, Ben Strome (Guice et al., 2018a) and Drumbeg (Fig. 2b) display Badcallian to Inverian folds that are cross-cut by Laxfordian shear zones and/ or Scourie Dykes. In contrast, the steeply-dipping (70-90°) Loch Eilean na Craoibhe Moire exhibits a NW-SE, Inverian/ Laxfordian trend that is cross-cut by Scourie Dykes and a suite of NE-SW-trending, likely Phanerozoic, faults (Fig. 2a). This variation can probably be attributed to the close proximity of the Loch Eilean na Craoibhe Moire Complex to the Laxford Shear Zone (Fig. 1), while the Ben Strome and Drumbeg Complexes are located further south. Moreover, while the ultramafic and mafic rocks occur, on average, in a 1:2 ratio, significant variation is observed between occurrences. The Loch Eilean na Craoibhe Moire and Drumbeg Complexes comprise more than 50 % ultramafic rocks, while the Ben Auskaird Complex contains 100 % mafic rocks. This variation is unlikely a function of the outcrop availability, as all the complexes are well-exposed.

In contrast to this group of complexes, the Loch an Daimh Mor Complex – located in the NW of the Central Region (Fig. 1) – is represented by a 500 m² area containing several irregularly-shaped pods predominantly comprising ultramafic rocks (Fig. 2c). The generally massive ultramafic rocks, which are

almost exclusively metaperidotite, are highly serpentinised (\pm talc), exhibit grey-brown weathered surfaces (Fig. 3e) and show mm-scale chromite in places. Metaperidotite is variably veined by separate carbonate- and orthopyroxene-rich veins, with the latter more numerous than the former (Faithfull et al., 2018). The orthopyroxene-dominated veins, which display sharp contacts with the surrounding ultramafic rocks, are 1-40 cm thick and contain centimetre-scale zircon crystals interpreted as associated with Inverian metasomatism (Faithfull et al., 2018). Adjacent metagabbro-dominated mafic rocks, which occur in association with intermediate gneiss, are poorly-exposed and locally contain coarse garnet. Importantly, the foliation in the surrounding TTG gneiss displays distinctive discordance with the lithological contacts on the map-scale (Fig. 2c).

In contrast to all previously described occurrences, the Geodh' nan Sgadan Complex – located less than 2 km SW of Loch an Daimh Mor (Fig. 1) – is a moderately-dipping, 15 m thick package of layered mafic rocks (Guice et al., 2018a; Fig. 2f). The Complex is underlain and overlain by TTG gneiss, with the gneissosity in the TTG parallel to the layering in the mafic rocks. Ultramafic rocks are absent, and the surrounding TTG gneiss contains a large number of centimetre-scale mafic pods that are possibly derived from the layered body. Layering in the plagioclase-rich mafic rocks is defined by millimetre-scale variation in the modal abundance of plagioclase, amphibole and pyroxene, with garnet restricted to rare, centimetre-scale horizons (Guice et al., 2018a). Such layering ranges from well-defined and laterally continuous on a scale of tens of metres to poorly-defined and chaotic (Fig. 3f).

ANALYTICAL INSTRUMENTATION AND METHODOLOGY

Bulk-rock geochemistry

All analysed samples were crushed and ground to a fine powder using the rock preparation facilities at Cardiff University (School of Earth and Ocean Sciences). Weathered surfaces were removed using a diamond-bladed rock saw, before samples were crushed using a Mn-steel jaw-crusher and ground

218 using an agate ball mill. Powdered samples were then ignited (at ~900°C) for 2 hours, with LOI
219 determined gravimetrically.

220 *Lithophile elements*

221 A sample mass of 0.1 g was accurately weighed and mixed with 0.6 g of Li metaborate flux in a Claisse
222 BIS! Pt-Rh crucible (see McDonald and Viljoen 2006 for full details). Approximately 0.5 mL of a Li iodide
223 solution was added as a non-wetting agent, before the mixture was fused over a propane burner on a
224 Claisse FLUXY (automated) fusion system. The mixture was subsequently poured into a Teflon beaker
225 containing 50 ml of 4 % HNO₃, where it was dissolved using a magnetic stirrer. Following dissolution
226 of all glass fragments, the solution was spiked with 1 mL of a 100 ppm Rh spike solution (for use as an
227 internal standard) and made up to 100 mL with 18.2 MΩ deionised water (McDonald and Viljoen,
228 2006). Samples were subsequently analysed for major and trace elements using ICP-OES and ICP-MS
229 respectively.

230 Standard reference materials and blanks were prepared and analysed using the methodology and
231 instrumentation described above, with the sample material omitted for the blanks. Accuracy was
232 constrained by analysis of a suite of international standard reference materials (see supplementary
233 material). Precision was constrained by duplicate analyses of ~5 % of samples and by conducting
234 repeat analyses of standards in different sample batches.

235 *Platinum-group elements and gold*

236 Samples were prepared by Ni sulphide fire assay and Te co-precipitation (fully described in: Huber et
237 al. 2001, McDonald and Viljoen 2006). Typically, 10 g of sample material (as ground rock powder;
238 method described above) is mixed with: 5 g of silica, 6 g of Na-carbonate, 12 g of borax, 0.9 g of sulphur
239 and 1.1 g of carbonyl-purified Ni. Reagents were thoroughly mixed before samples were transferred
240 to fire-clay crucibles before being fired at 1050°C for 90 minutes. Buttons were dissolved using
241 concentrated HCl, with co-precipitation achieved using Te and SnCl₂. The filtered residues were
242 digested using 3 ml of concentrated HNO₃ and 4 ml of concentrated HCl in sealed 15 ml Saville screw-

top Teflon vials. After the residue had dissolved, the liquid contents were transferred to 50 ml volumetric flasks, spiked with a 2.5 ppm Tl spike (for use as an internal standard) and made up to 50 ml with 18.2 MΩ deionised water. Solutions were then analysed for PGE and Au using an ICP-MS system at Cardiff University.

Standard reference materials and blanks were prepared and analysed using the methodology and instrumentation described above, with the sample material omitted for the blanks, for which a 10 g Si mass was used. Accuracy was constrained by analysis of a suite of international standard reference materials (see supplementary material). Precision was constrained by conducting duplicate analyses of ~10 % of samples, and by conducting repeat analyses of standards in different sample batches.

Element mapping

Detailed petrographic assessment by element mapping used a Zeiss Sigma HD Field Emission Gun A-SEM (A-SEM) equipped with two Oxford Instruments 150 mm² Energy Dispersive X-ray Spectrometry (EDS) detectors at the School of Earth and Ocean Sciences, Cardiff University. Operating conditions were set at 20 kV and aperture size to 120 μm, with a nominal beam current of 4 nA and working distance of 8.9 mm. Using Aztec software, maps were acquired at 100 to 150× magnifications, with resulting pixel sizes ranging from 10 to 22 μm, depending on the resolution of acquired spectral images. A process time of 1 μs was used in conjunction with a pixel dwell time of 3000–6000 μs. Element maps were then background correlated and element overlaps deconvolved using Aztec software, before modal mineralogy was calculated from relative element concentrations using the analyse phases algorithm in Aztec. Boundary tolerance and grouping level were set at 2 and 1 respectively, with any unassigned pixels (typically < 5 %) discarded from the modal mineralogy.

PETROGRAPHY

A total of 62 polished thin sections (including 37 ultramafic samples and 25 mafic samples) from the 12 studied complexes were made at Cardiff University and subject to petrographic assessment.

Further to basic optical microscopy, 33 samples were subject to detailed petrographic assessment by element mapping using an A-SEM. Where possible, these maps were utilised to estimate modal mineral proportions, with details of the instrumentation and methodology utilised described above. The location (GPS coordinates in British National Grid) and modal mineral proportion of each sample is included in Table 1 (ultramafic rocks) and Table 2 (mafic rocks). These tables also detail both the average and range of modal mineral proportions for each ultramafic-mafic complex, with the sections below summarising the broader petrographic features observed in the ultramafic and mafic lithologies studied.

Ultramafic rocks

The modal mineral proportions of the ultramafic rocks assessed vary between and within complexes (Table 1), but the samples exhibit several consistent mineralogical and textural features (Fig. 4a-c). In terms of basic mineralogy, the ultramafic rocks comprise (in variable proportions): olivine, serpentine, orthopyroxene, clinopyroxene, amphibole, spinel and accessory sulphide phases (Table 1). Olivine is rarely preserved as millimetre-scale, subhedral grains or remnants within masses of fine-grained serpentine (\pm magnetite). Clino- and ortho-pyroxene, which are euhedral and 0.5 to 3.5 mm in diameter, are variably replaced by fine-grained (< 0.2 mm diameter) amphibole, with orthopyroxene dominant over clinopyroxene. Late retrogressive amphibolitisation of pyroxene ranges from near-absent (occurring as rare rims on individual pyroxene grains; to near-complete within individual thin sections). Older, high-grade metamorphic pargasitic, amphibole (pale green in thin sections) occurs as < 2.1 mm diameter, generally subhedral grains, with these grains forming 120° triple junctions. Spinel occurs as euhedral to subhedral grains < 3.5 mm in diameter, while pentlandite, pyrrhotite and chalcopyrite occur rarely, as anhedral to euhedral grains < 0.2 mm diameter.

Mafic rocks

The mafic rocks from the Ben Strome, Ben Auskaird and Gorm Chnoc Complexes are mineralogically and texturally comparable (Table 2), while the Geodh' nan Sgadan Complex is texturally distinct (Fig.

4d-f). In the Ben Strome, Ben Auskaird and Gorm Chnoc Complexes (Fig. 4d-e), pyroxene is subhedral to anhedral, 0.5 to 2.5 mm in diameter, and variably replaced by fine-grained (< 0.2 mm diameter) amphibole, with clinopyroxene dominant over orthopyroxene. Amphibole (clear in thin section) also occurs as 0.2 to 2 mm diameter grains that commonly display pleochroism and 120° triple junctions. Garnet occurs as millimetre- to centimetre-scale, anhedral to subhedral grains that exhibit significant retrogression to plagioclase (\pm amphibole), commonly as rims. Magnetite is the dominant oxide phase, forming subhedral grains < 0.3 mm in diameter. Ilmenite is rare, but where present comprise < 7 % of individual samples (Table 2).

As described by Guice et al. (2018a), pyroxene in the Geodh' nan Sgadan Complex is generally 0.2 to 0.6 mm in diameter and subhedral to euhedral (fig. 4f). Pyroxene exhibits alteration to amphibole, which forms a fine-grained groundmass in most samples. Amphibole also exists as 0.2 to 0.5 mm diameter subhedral grains that display 120° triple junctions. Plagioclase feldspar is 0.4 to 0.6 mm in diameter and subhedral, with rare triple junctions and some amphibole replacement.

BULK-ROCK GEOCHEMISTRY

From the 12 studied ultramafic-mafic complexes, a total of 45 ultramafic and 27 mafic rocks were analysed for bulk-rock major and trace element geochemistry, with a smaller sample set analysed for PGE and Au (44 ultramafic and 6 mafic samples). Details of the analytical instrumentation and methodology are described above, with the precision calculations, analyses of standard reference material, and raw data included in the supplementary material.

Table 3 summarises the geochemical characteristics of each complex by outlining the range of key major element abundances, trace element ratios and PGE ratios. In-line with the aims of this paper, Figures 5-8 include comparisons with: (a) the Ben Strome ultramafic rocks considered by Guice et al. (2018b) to most closely resemble primary compositions; (b) the Ben Strome mafic rocks presented here; and (c) abyssal peridotites and ultramafic mantle rocks (data from: Godard et al., 2008, 2000; Paulick et al., 2006). Given the distinctive field characteristics shown by the Loch an Daimh Mor and

317 Geodh' nan Sgadan Complexes, these occurrences are distinguished in Figure 5, while each complex
318 is considered separately in Figures 6-8.

319 ***Major and minor elements***

320 As detailed fully in Table 3, the analysed ultramafic rocks contain 17 to 42 wt. % MgO, up to 0.9 wt. %
321 TiO₂ and 2 to 4 wt. % Al₂O₃, while the mafic rocks contain 3 to 21 wt. % MgO, less than 3 % TiO₂ and 8
322 to 20 wt. % Al₂O₃.

323 As shown on bulk-rock bivariate plots, MgO in the ultramafic rocks exhibits moderate to strong
324 negative correlations ($R^2 = > 0.4$) with TiO₂, Al₂O₃ and CaO, weak negative correlations ($R^2 = 0.1 - 0.4$)
325 with Na₂O, a weak positive correlation with NiO and no correlation with SiO₂, Cr₂O₃ and Fe₂O₃ (Table
326 3; Fig. 5). With the exception of the Loch an Daimh Mor Complex, the ultramafic rocks from all other
327 complexes show consistent overlap with the field for Ben Strome Complex ultramafic rocks (Table 3;
328 Fig. 5). Relative to this group, the Loch an Daimh Mor Complex exhibits SiO₂ and NiO enrichment,
329 alongside Cr₂O₃, Fe₂O₃ Al₂O₃ and CaO depletion (Table 3; Fig. 5). These samples show partial overlap
330 with the field for ophiolites and abyssal peridotites on MgO versus SiO₂, Fe₂O₃, CaO, Na₂O, NiO and
331 Cr₂O₃ plots (Fig. 5), while the majority of the ultramafic rocks show no overlap with this field.

332 Distinctive compositional trends are not present within the mafic samples, but these rocks form a part
333 of linear trends when considering both ultramafic and mafic lithologies. MgO displays a moderate to
334 strong negative correlation ($R^2 = > 0.4$) with Al₂O₃, CaO and Na₂O, a weak negative correlation ($R^2 =$
335 $0.1 - 0.4$) with SiO₂ and Fe₂O₃, a moderate positive correlation with Cr₂O₃, and a weak positive
336 correlation with NiO (Fig. 5). The analysed mafic rocks from the Ben Auskaird, Drumbeg, Geodh' nan
337 Sgadan and Gorm Chnoc Complexes generally overlap with the Ben Strome field, although the Geodh'
338 nan Sgadan and Gorm Chnoc Complexes show minor relative depletion in TiO₂ and Fe₂O₂ (Fig. 5).

339 **Trace elements**

340 *Ultramafic rocks*

341 On chondrite-normalised REE plots (Fig. 6), the ultramafic rocks from the Ben Strome Complex
342 considered to most closely resemble primary compositions (Guice et al., 2018b) exhibit flat overall
343 patterns ($[La/Lu]_N = 0.5 - 2$), with chondrite-normalised REE abundances ranging from 1.1 to 8.1.
344 Similarly flat REE patterns are shown by the majority of ultramafic rocks from the Achiltibuie ($[La/Lu]_N$
345 $= 0.7 - 2.3$), Drumbeg ($[La/Lu]_N = 0.6 - 1.9$), Gorm Chnoc ($[La/Lu]_N = 1.8 - 2.1$), Loch Eilean na Craoibhe
346 Moire ($[La/Lu]_N = 1.0 - 2.9$), North Scourie Bay ($[La/Lu]_N = 2.7$) and Scouriemore ($[La/Lu]_N = 0.8 - 5$)
347 Complexes, with these rocks showing near-complete overlap with the Ben Strome Complex ultramafic
348 rocks (Table 3; Fig. 6). Other complexes exhibit REE patterns that can be distinguished from those of
349 the Ben Strome rocks. The Achmelvich Complex samples exhibit positively sloping LREE ($[La/Sm]_N =$
350 $0.3 - 0.5$), with relatively flat MREE and HREE that overlap with the Ben Strome field (Fig. 6b). The
351 Ben Dreavie samples show significant LREE enrichment ($[La/Sm]_N = 6.1 - 9.7$), but overlap with the
352 Ben Strome Complex in terms of MREE and HREE (Fig. 6d). The Loch an Daimh Mor Complex is the
353 most distinctive, exhibiting mild depletion in MREE and HREE relative to the Ben Strome Complex (0.8
354 $\text{to } 2.9 \times \text{chondrite}$), alongside negatively sloping LREE ($[La/Sm]_N = 1.5 - 3.2$). All complexes show
355 significant enrichment of all REE relative to the field for ophiolites and oceanic peridotites (Fig. 6).

356 On primitive mantle-normalised trace element plots (Fig. 7), the ultramafic rocks from the Ben Strome
357 Complex generally show flat overall patterns ($[Nb/Yb]_N = 0.4 - 3.9$) with no negative Nb-Ta anomalies
358 and normalised trace element abundances between 0.2 and 15. Similarly flat trace element patterns
359 are shown by the majority of ultramafic rocks from the Achiltibuie ($[Nb/Yb]_N = 0.8 - 2.6$), Achmelvich
360 ($[Nb/Yb]_N = 0.4 - 2.5$), Drumbeg ($[Nb/Yb]_N = 0.6 - 1.2$), Loch Eilean na Craoibhe Moire ($[Nb/Yb]_N = 0.4$
361 $- 2.9$), North Scourie Bay ($[Nb/Yb]_N = 1.2$) and Scouriemore ($[Nb/Yb]_N = 0.6 - 2.2$) Complexes, with
362 near-complete overlap with the Ben Strome field. The Ben Dreavie Complex (Fig. 7d) exhibits
363 significant enrichment in Ba, La, Ce, Sr, Nd and Sm ($[La/Ta]_N = 6 - 32$) relative to this field, alongside

associated negative Nb-Ta-Zr-Hf-Ti anomalies. Such patterns are comparable to those Ben Strome ultramafic rocks considered by Guice et al. (2018b) to have experienced LREE enrichment by metasomatism associated with H₂O/CO₂-rich fluids during amphibolitisation. The Gorm Chnoc Complex ultramafic rocks (Fig. 7h) also display negative Nb-Ta-Zr-Hf anomalies ($[\text{Nb}/\text{Yb}]_{\text{N}} = 0.5 - 0.6$; $[\text{La}/\text{Ta}]_{\text{N}} = 2.8 - 3.2$), but, in comparison to Ben Dreavie, are lacking the associated enrichment of the LREE and elements more typically considered fluid mobile (e.g., Ba). The Loch an Daimh Mor Complex ultramafic rocks (Fig. 7i) exhibit overall flat patterns ($[\text{Nb}/\text{Yb}]_{\text{N}} = 0.5 - 2.2$) and positive LREE anomalies ($[\text{La}/\text{Ta}]_{\text{N}} = 0.2$ to 0.9), with mild depletion in the most incompatible (Rb to Nb) and compatible (Ti to Lu) elements.

Mafic rocks

On chondrite-normalised REE plots (Fig. 6), the mafic rocks from the Ben Strome Complex exhibit chondrite-normalised values between 4 and 62, with some mildly positive slopes and some mildly negative slopes ($[\text{La}/\text{Lu}]_{\text{N}} = 0.3 - 8$). The Ben Auskaird mafic rocks (Fig. 6c) show minor enrichment in the HREE and MREE relative to Ben Strome, but otherwise exhibit similar, positively sloping patterns ($[\text{La}/\text{Sm}]_{\text{N}} = 1.3 - 2.5$; $[\text{La}/\text{Lu}]_{\text{N}} = 2.0 - 3.1$). The one Drumbeg Complex sample shows a positively sloping pattern ($[\text{La}/\text{Sm}]_{\text{N}} = 1.5$; $[\text{La}/\text{Lu}]_{\text{N}} = 7$), alongside mild enrichment in almost all REE. The two samples from the Gorm Chnoc Complex (Fig. 6h) show flat MREE and HREE patterns, negatively sloping LREE ($[\text{La}/\text{Sm}]_{\text{N}} = 0.6 - 0.8$; $[\text{La}/\text{Lu}]_{\text{N}} = 0.6 - 0.9$) and mild depletion in all REE relative to the Ben Strome Complex. The Geodh' nan Sgadan Complex samples show the greatest distinction from the Ben Strome Complex, showing a broad range in REE contents (2 to 126 x chondrite). These rocks exhibit relatively flat MREE and HREE, alongside negatively sloping LREE ($[\text{La}/\text{Sm}]_{\text{N}} = 1.7 - 2.8$).

On primitive mantle-normalised trace element plots (Fig. 7), the mafic rocks from the Ben Strome Complex generally exhibit flat patterns ($[\text{Nb}/\text{Yb}]_{\text{N}} = 0.3 - 1.9$) that are punctuated by mild negative Th-U-Zr-Hf anomalies and mild positive Rb-Ba-Sr anomalies. The Ben Auskaird mafic rocks display a comparable pattern ($[\text{Nb}/\text{Yb}]_{\text{N}} = 2.2$), but with a negative Sr anomaly and mild enrichment in some of

the most incompatible (Ba, Th) and compatible (Tb to Lu) elements. Similarly, while the one Drumbeg Complex sample (Fig. 7f) shows a flat pattern ($[\text{Nb}/\text{Yb}]_N = 0.8$) and significant overlap with the Ben Strome field, this sample shows positive La-Ce-Sr-Nd anomalies. The Gorm Chnoc mafic rocks (Fig. 7h) display mild-moderate trace element depletion relative to the Ben Strome Complex, with pronounced negative Nb-Ta-Zr-Hf anomalies ($[\text{Nb}/\text{Yb}]_N = 0.2 - 0.3$; $[\text{La}/\text{Ta}]_N = 2.0 - 5.2$). Despite showing a significantly larger range in trace element abundances when compared to the Ben Strome Complex, the Geodh' nan Sgadan Complex also displays flat trace element patterns ($[\text{Nb}/\text{Yb}]_N = 0.5 - 1.5$), while selected samples show enrichment in Rb and Ba (Fig. 7g).

Platinum-group elements and gold

Ultramafic rocks

On chondrite-normalised PGE (+Au) plots, the Ben Strome Complex ultramafic rocks (Fig. 8) exhibit mild to moderately fractionated PGE patterns ($[\text{Pd}/\text{Ir}]_N = 2 - 33$), with positively sloping Ir-group PGE (IPGE) with $[\text{Ru}/\text{Os}]_N = 1.4 - 3.9$ and near-flat to positively sloping Pd-group PGE (PPGE) where $[\text{Pd}/\text{Rh}]_N = 0.7 - 5.1$. This overall PGE fractionation is replicated by the Achiltibuie ($[\text{Pd}/\text{Ir}]_N = 4.8 - 9.3$), Achmelvich ($[\text{Pd}/\text{Ir}]_N = 6.0 - 10.6$), Ben Dreavie ($[\text{Pd}/\text{Ir}]_N = 7.2 - 15.6$), Drumbeg ($[\text{Pd}/\text{Ir}]_N = 3.5 - 8.4$), Loch Eilean na Craoibhe Moire ($[\text{Pd}/\text{Ir}]_N = 1.6 - 12.9$), North Scourie Bay ($[\text{Pd}/\text{Ir}]_N = 10.3$) and Scouriemore ($[\text{Pd}/\text{Ir}]_N = 1.9 - 25.5$) Complexes (Fig. 8). The ultramafic rocks from the Gorm Chnoc and Loch an Daimh Mor Complexes, however, show patterns that are distinctive from this group of complexes. The Gorm Chnoc samples are strongly fractionated ($[\text{Pd}/\text{Ir}]_N = 117 - 124$) and relatively depleted in IPGE (Fig. 8h). The Loch an Daimh Mor Complex samples can be subdivided into two groups. The first subgroup (n=3) shows flat to negatively sloping PGE patterns ($[\text{Pd}/\text{Ir}]_N = 0.2 - 1.2$), negatively sloping IPGE ($[\text{Ru}/\text{Os}]_N = 0.3 - 0.5$) and negatively sloping to flat PPGE ($[\text{Pd}/\text{Rh}]_N = 0.3 - 1.6$). The second subgroup (n=3) exhibits positively sloping PGE patterns ($[\text{Pd}/\text{Ir}]_N = 2.2 - 4.2$), positively sloping to flat IPGE ($[\text{Ru}/\text{Os}]_N = 1.1 - 9.9$) and positively sloping to flat PPGE ($[\text{Pd}/\text{Rh}]_N = 1.6 - 3.5$).

413 *Mafic rocks*

414 The Ben Strome Complex mafic rocks (Fig. 8) exhibit moderately fractionated PGE patterns ($[\text{Pd}/\text{Ir}]_N =$
415 $24 - 46$), with this pattern broadly consistent with the Ben Auskaird samples ($[\text{Pd}/\text{Ir}]_N = 18 - 44$; Fig.
416 8c). The Geodh' nan Sgadan mafic rocks (Fig. 8g) also exhibit broadly fractionated patterns ($[\text{Pd}/\text{Ir}]_N =$
417 $8 - 24$), but, in contrast to Ben Strome, this pattern comprises positively sloping IPGE ($[\text{Ru}/\text{Os}]_N = 10 -$
418 25) and negatively sloping PPGE ($[\text{Pd}/\text{Rh}]_N = 0.3 - 0.7$).

419 **DISCUSSION**

420 The Central Region LGC records a protracted magmatic and metamorphic history that includes at least
421 3 peaks of amphibolite- to granulite-facies metamorphism. This tectonothermal history, which spans
422 1 billion years, is associated with polyphase deformation, metasomatism, and partial melting of felsic,
423 intermediate and some mafic lithologies (Johnson et al., 2012; Park et al., 2002). As noted by Johnson
424 et al. (2016), this generates inherent ambiguity when attempting to unpick primary geochemical
425 signatures and interpret the origin and geodynamic significance of ultramafic-mafic rocks. Moreover,
426 as demonstrated by Guice et al. (2018b), metasomatic effects in the LGC can be both cryptic and
427 extremely localised. These authors show that the LREE – elements typically considered relatively
428 immobile – were enriched in selected samples during interaction with CO_2 - and H_2O -rich fluids,
429 generating apparent negative high field strength element (HFSE) anomalies which, out of context, may
430 have been interpreted as evidence for subduction-related magmatism.

431 This local variation in deformation, metamorphism and metasomatism is considered throughout the
432 succeeding sections, which aim to unravel the primary geological and geochemical characteristics of
433 the ultramafic-mafic complexes studied. As stated in the Introduction, the paper specifically aims to:
434 (i) examine the validity of the layered intrusion hypothesis (“Ben Strome model”) for other ultramafic-
435 mafic complexes in the Central Region LGC; and (ii) if/where this hypothesis fails, assess the possibility
436 that fragments of Archaean mantle may be preserved within this portion of the North Atlantic Craton.

Aim (i) is addressed in the first section of the discussion, with the second and third sections tackling aim (ii). Reference is made throughout to Table 3, which summarises the geochemical features of each ultramafic-mafic complex studied.

The Ben Strome Complex: unique occurrence or type locality?

Seven of the studied complexes – Achiltibuie, Achmelvich, Ben Auskaird, Drumbeg, Loch Eilean na Craoibhe Moire, North Scourie Bay and Scouriemore – display field relationships and geochemical characteristics that are near-identical to those of the Ben Strome Complex (Table 3). Such field characteristics include: a predominance of metapyroxenite in the ultramafic portions; pronounced mm- to m-scale layering in ultramafic lithologies (Fig. 3a-c); relatively discrete layering in the mafic rocks that is defined by the proportions of garnet, pyroxene and plagioclase (Fig. 3d); and consistent parallelism between the layering in the ultramafic-mafic rocks, foliation in the TTG gneiss, and lithological contacts, irrespective of the dominant structural regime (Fig. 2). These common field observations are compounded by the consistent geochemical characteristics shown by this group of complexes (Table 3; Figs. 5-8), which includes: flat chondrite-normalised REE patterns for ultramafic rocks (Fig. 6); negatively- to positively-sloping, chondrite-normalised REE patterns for mafic rocks (Fig. 6); flat primitive mantle-normalised trace elements for ultramafic rocks (Fig. 7); mildly- to moderately-fractionated PGE patterns for ultramafic rocks (Fig. 8); and moderately fractionated PGE patterns for mafic rocks (Fig. 8). These consistent salient features indicate that this group of complexes likely share a common and broadly contemporaneous origin with the Ben Strome Complex.

Based on field observations, detailed mapping and spinel mineral chemistry, Guice et al. (2018a) suggested that the Ben Strome Complex (and therefore this group of complexes collectively) most likely represents a layered intrusion(s). The field characteristics reported here support this hypothesis, with these other occurrences also exhibiting field features characteristic of layered intrusions (Namur et al. 2015), such as: gradational contacts between ultramafic and mafic units; gradational contacts between metaperidotites and metapyroxenite layers in the ultramafic portions; gradational variation

in modal mineral proportions within individual layers; multiple ultramafic and mafic packages occurring within single continuous successions (known as “megacyclic units”; Fig. 2); and truncation of layers on the centimetre- to metre-scale (Fig. 3b-c). This hypothesis is also supported by the geochemical data presented in this paper, with ultramafic and mafic rocks from the 8 complexes (including Ben Strome) collectively displaying: fractionated trends on major element bivariate plots (Fig. 5); and mild- to moderately- fractionated PGE patterns that are typical of layered intrusions (Barnes et al., 1985; Power et al., 2000).

As addressed by Guice et al. (2018a), a layered intrusion interpretation does not, however, solve the crucial age relationship quandary. The field mapping presented in Figure 2 (this study) and by Guice et al. (2018a) highlights the extremely varied and seemingly chaotic map-scale morphologies displayed by this group of complexes. On the one hand, this observation may be used as evidence supporting an interpretation whereby these complexes pre-date the TTG magmas. However, unambiguous field evidence in the form of cross-cutting relationships are strikingly absent. Moreover, none of the complexes show a spatial association with centimetre- to metre-scale ultramafic-mafic pods in the surrounding TTG gneiss, which are used to infer such age relationships elsewhere in the North Atlantic Craton (Whitehouse and Fedo, 2003). Rather than representing a chaotic distribution caused by fragmentation by TTG magmas, the morphologies displayed by these complexes can instead be attributed to local variation in the predominant structural regime. For example, the Ben Strome and Drumbeg (Fig. 2b) Complexes show Badcallian to Inverian folds that are cross-cut by both Scourie Dykes and Laxfordian shear zones. In contrast, the Loch Eilean na Craoibhe Moire Complex (Fig. 2a), which is located less than 1 km south of the Laxford Shear Zone, show a steeply-dipping, Laxfordian trend that is cross-cut by Scourie Dykes and NE-SW-trending Phanerozoic faults. This strongly suggests that the spatial distribution of ultramafic-mafic rocks reflects the polyphase deformation, rather than primary magmatic fragmentation by TTG magmas.

In the absence of unambiguous cross-cutting relationships, a simple model is proposed, whereby this suite of complexes represent several layered intrusions that were emplaced *into* TTG prior to polyphase deformation and metamorphism (Guice et al., 2018a). It should be noted that because all observed contacts between ultramafic-mafic rocks and the surrounding TTG gneiss are tectonic, such intrusions were not necessarily emplaced into the specific felsic rocks with which they are today juxtaposed. This hypothesis is consistent with the Re-Os isotopic study of Burton et al. (2000) and with recent zircon geochronology conducted by Taylor et al. (2020). In this scenario, it is likely that some of the adjacent complexes studied here (i.e., Scouriemore and North Scourie Bay; or Ben Strome and Ben Dreavie) may represent the dismembered fragments of originally continuous layered intrusions (Fig. 9). To answer the question posed in the title of this subsection, the Ben Strome Complex can be considered the type locality for this type of ultramafic-mafic body in the Central Region LGC. This finding represents a significant re-evaluation of the LGC's magmatic evolution, with at least 8 ultramafic-mafic complexes suggested to post-date, rather than pre-date, the TTG magmas, and is outlined in Figure 9.

Affiliation of the other ultramafic-mafic bodies

The remaining 4 complexes – Ben Dreavie, Geodh' nan Sgadan, Gorm Chnoc and Loch an Daimh Mor – exhibit some distinction from the group of Ben Strome-type complexes described above. This section assesses whether such variation can be attributed to a distinctive origin, or whether local variation in metamorphism, metasomatism and/or deformation is instead responsible. We aim to test the hypothesis that the LGC records multiple phases of Archaean ultramafic-mafic magmatism (Guice et al., 2018a; Rollinson and Gravestock, 2012).

Ben Dreavie: a Ben Strome-type complex

The Ben Dreavie Complex is comparable to the Ben Strome-type complexes in terms of field relationships, major and minor-element geochemistry (Fig. 5) and PGE geochemistry (Fig 8; Table 3). For example, distinctive layering is prominent in the metapyroxenite-dominated ultramafic rocks,

comparable ranges are observed in all major and minor elements, and the PGE patterns are fractionated ($[\text{Pd}/\text{Ir}]_{\text{N}} = 3 - 8$). In contrast to the Ben Strome-type complexes, the small number of ultramafic rocks from the complex ($n=2$) display distinctive chondrite-normalised REE and primitive mantle-normalised trace element patterns, with LREE enrichment ($[\text{La}/\text{Ta}]_{\text{N}} = 6 - 32$) and associated HFSE anomalies (Figs. 6-7; Table 3). Despite this, the primitive mantle-normalised Nb/Yb ratios are near-identical ($[\text{Nb}/\text{Yb}]_{\text{N}} = 0.5 - 1.6$) to those of the Ben Strome Complex ($[\text{Nb}/\text{Yb}]_{\text{N}} = 0.4 - 3.9$), with the Ben Dreavie samples showing almost complete overlap with this field (Fig. 7). Moreover, this trace element pattern, whereby apparent negative HFSE anomalies are associated with LREE enrichment, strongly resembles those described in selected samples from the Ben Strome Complex (Guice et al., 2018b), with localised LREE enrichment by metasomatism associated with H_2O and CO_2 -rich fluids during amphibolitisation. Corresponding enrichment of Ba and Sr in the Ben Dreavie samples – typically fluid mobile elements – suggests that similar, secondary, processes may have also generated the anomalies in this instance, particularly given the proximal location of the Ben Strome Complex (Fig. 1). While this hypothesis requires assessment by more detailed investigation, the simplest explanation is that the Ben Dreavie Complex shares a common, layered intrusion, origin with the Ben Strome-type complexes, with the only distinguishing feature – LREE enrichment – likely associated with local metasomatic processes.

Loch an Daimh Mor: evidence for multiple phases of magmatism in the LGC

The Loch an Daimh Mor Complex is distinguished from the Ben Strome-type complexes based on several field observations and geochemical characteristics, including (Table 3): the predominance of metaperidotite (Figs. 2 and 3); restriction of metapyroxenite to late, cross-cutting veins, rather than layers (Figs. 2 and 3); occurrence as irregularly-shaped, decimetre-scale pods (Fig. 2); local abundance of Cr-spinel; the map-scale discordance between pod margins and the foliation in the TTG (Fig. 2); the relative SiO_2 and NiO enrichment and Cr_2O_3 , Fe_2O_3 , Al_2O_3 and CaO depletion (Fig. 5); HREE-depleted, LREE-enriched REE patterns (Fig. 6); depletion of the most compatible and most incompatible elements on primitive mantle-normalised trace-element plots (Fig. 7); and the flat to negatively

sloping PGE patterns shown by a selection of samples (Fig. 8). It is difficult to envisage a scenario in which all these diverse features can be explained by metamorphism, metasomatism and deformation of an ultramafic-mafic complex that originally resembled Ben Strome. Why, for example, are the ultramafic rocks composed almost exclusively of metaperidotite, when this lithology is extremely rare in the Ben Strome-type complexes? How would a metasomatic process(es) enrich the Loch an Daimh Mor rocks in SiO_2 , NiO and the IPGE, whilst depleting them in Cr_2O_3 , Fe_2O_3 , Al_2O_3 , CaO and the HREE? Whilst impossible to discount completely without conducting detailed investigations, it appears highly unlikely, based on the evidence presented here, that the characteristics described above can be attributed to a unique suite of metamorphic and metasomatic processes. Instead, we consider it most likely that the Loch an Daimh Mor Complex records an origin distinctive from the Ben Strome-type complexes, supporting the hypothesis that the LGC records multiple petrogenetically distinct suites of Archaean ultramafic-mafic magmatism (Fig. 9). The specific origin is discussed further in a subsequent section.

Geodh' nan Sgadan and Gorm Chnoc: unknown affiliation

The Geodh' nan Sgadan Complex is distinguished from the Ben Strome-type complexes based on: extremely prominent and varied layering in the mafic rocks; an abundance of centimetre-scale pods in the surrounding TTG gneiss; rarity and restriction of garnet to rare, centimetre-scale layers; minor depletion in TiO_2 and Fe_2O_3 on major element bivariate plots (Fig. 5); a relatively broad range of chondrite-normalised REE and primitive mantle-normalised trace element abundances (Figs. 6-7); and flat PPGE patterns (Rh-Pd; Fig. 8). Despite this, these rocks show significant overlap with the Ben Strome Complex on almost all major and minor-element bivariate plots (Fig. 5), and show broad REE and trace-element patterns that are roughly comparable to this field (Figs. 6-7). It is possible that some of the aforementioned distinctions are a consequence of the Geodh' nan Sgadan Complex comprising 100 % mafic rocks, which are relatively susceptible to the high-grade metamorphism and associated partial melting. However, this does not explain the presence of the centimetre-scale pods in the surrounding TTG, which are never observed in association with the Ben Strome-type complexes. We

therefore suggest that the Geodh' nan Sgadan Complex could represent a different, perhaps older, protolith that fragmented into the TTG during deformation, but further evidence is required.

The Gorm Chnoc Complex is comparable to the Ben Strome-type complexes in terms of field relationships, major element geochemistry and REE geochemistry, but can be distinguished from this group based on the primitive mantle-normalised trace element patterns (Fig. 7) and the extremely fractionated ($[Pd/IR]_N = 117 - 124$) chondrite-normalised PGE patterns (Fig. 8; Table 3). On trace element plots, the Gorm Chnoc ultramafic rocks display negative Nb-Ta-Zr-Hf anomalies, but, unlike Ben Dreavie, these samples lack the associated enrichment of LREE and elements typically considered fluid mobile (e.g., Ba), suggesting these anomalies could be primary. This, combined with the distinctive PGE patterns, implies that the Gorm Chnoc Complex is distinct from both the Ben Strome-type and Loch an Daimh Mor complexes. However, the consistency in terms of field relationships, major element geochemistry and REE geochemistry questions this assertion. Moreover, its location within the Laxford Shear Zone requires caution, with metasomatism highly likely in this region. Ultimately, based on the current data, it is difficult definitively determine whether the Gorm Chnoc Complex represents a distinct magmatic protolith, or whether it is a more intensely metasomatised equivalent of the Ben Strome-type Complexes.

Loch an Daimh Mor: a fragment of Archaean mantle?

On the map-scale, the Loch an Daimh Mor Complex occurs as large pods within the TTG gneiss, displaying significant discordance between the gneissose foliation and lithological contacts (Fig. 2c). Although there is no direct evidence of TTG cross-cutting the ultramafic rocks, this map-scale morphology and associated discordance hints that this complex may pre-date the TTG, as previously suggested for all of the ultramafic-mafic complexes in the LGC (Park et al., 2002; Sills, 1981). Given the reported crystallisation ages for the Central Region TTG, which range from 3.1 to 2.8 Ga and are based on U-Pb zircon geochronology (e.g., Kinny et al., 2005; Kinny and Friend, 1997; Love et al., 2010; MacDonald et al., 2015), a precise minimum age is impossible to reconcile for this complex. If the

588 outlined age relationship is correct, these ultramafic rocks must be at least 2.8 Ga (based on the
589 youngest reported crystallisation age for TTG protoliths in the Central Region LGC), but could have a
590 minimum age of 3.05 Ga. This is dependent upon the crystallisation age of the TTG gneiss that are
591 immediately adjacent to the Loch an Daimh Mor Complex, which have not yet been subject to U-Pb
592 zircon geochronology.

593 Using the criteria developed by Rollinson (2007), we here test the possibility that the Loch an Daimh
594 Mor Complex represent a fragment of Archaean mantle. Further to Figures 6, 7 and 8, which include
595 a comparison to oceanic residue, Figure 10 utilises the Mg/Si versus Al/Si and chondrite-normalised
596 Yb versus Ce/Sm plots. The Loch an Daimh Mor samples are compared to: abyssal peridotites, fore-
597 arc and sub-arc serpentinites, the Oman Ophiolite; orogenic peridotites; and, for a comparison to
598 ultramafic rocks produced by very different mantle-melting processes, komatiites. The other
599 complexes assessed as part of this study are also plotted for reference, with these rocks generally
600 plotting well outside of the field for abyssal peridotites and overlapping with the komatiites field on
601 the Al/Si versus Mg/Si plot (Fig. 10a). Moreover, on the chondrite-normalised Yb versus Ce/Sm plot,
602 the samples from the other studied complexes largely plot outside of the variety of mantle fields
603 included for reference (Fig. 10b). As outlined in the introduction to this discussion, the complex
604 tectonothermal history experienced by the LGC has likely resulted in (often cryptic) element mobility
605 that can only be constrained by detailed investigations of individual localities (Guice et al., 2018b;
606 Rollinson and Gravestock, 2012). Consequently, these plots should be treated with caution.

607 For the Loch an Daimh Mor Complex ultramafic rocks, the flat to negatively sloping chondrite-
608 normalised PGE patterns are comparable to those displayed by the mantle portions of ophiolites
609 (Barnes et al., 1985). This similarity is also observed on the Al/Si versus Mg/Si plots, on which 4 of the
610 5 samples fall within the abyssal peridotites field (Fig. 10a), and on the chondrite-normalised Yb versus
611 Ce/Sm plot, where the samples overlap with the orogenic peridotites field (Fig. 10b). However, this
612 geochemical comparison is contradicted by the chondrite-normalised REE abundances, which are 1-2

orders of magnitude greater than those for residual mantle rocks (Godard et al., 2008, 2000; Paulick et al., 2006; Fig. 6). While it is possible that these REE concentrations reflect mantle metasomatism and re-fertilisation of Archaean mantle, this interpretation requires a huge leap of faith based on the data presented here, particularly given the potentially profound implications for Archaean geodynamic regimes. Ultimately, the Loch an Daimh Mor Complex represents the strongest candidate for Archaean mantle yet discovered in the LGC, but further investigation is required to rigorously test this interpretation.

CONCLUSIONS

1. A suite of 8 ultramafic-mafic complexes – Achiltibuie, Achmelvich, Ben Auskaird, Ben Dreavie, Drumbeg Loch Eilean na Craoibhe Moire, North Scourie Bay and Scouriemore – share a common origin with the Ben Strome Complex, displaying consistent field relationships and geochemical characteristics. These Ben Strome-type complexes likely represent a suite of layered intrusions that were emplaced into the TTG prior to polyphase deformation and metamorphism. This finding is a significant re-evaluation of the LGC's magmatic evolution, with the majority of ultramafic-mafic bodies not predating the TTG, as previously assumed.

2. One ultramafic-mafic complex – Loch an Daimh Mor – is considered to unequivocally record an origin distinctive from that of the Ben Strome-type complexes, supporting the hypothesis that the LGC records multiple phases of petrogenetically and temporally distinct Archaean ultramafic-mafic magmatism. This demonstrates that ultramafic-mafic rocks in Archaean cratons, which are sometimes assumed to share a common origin, may record temporal snapshots of specific Archaean processes that can be used to reconstruct processes of cratonisation. The Loch an Daimh Mor Complex represents the strongest candidate for Archaean mantle yet discovered in the LGC, displaying some geochemical characteristics that resemble abyssal and orogenic peridotites.

ACKNOWLEDGEMENTS AND FUNDING

G.L.G. would like to thank The Society of Economic Geologists (Graduate Fellowship Award) and The Geological Society (Timothy Jefferson Fund) for generous bursaries that provided funding for the fieldwork upon which this research is based. G.L.G. would also like to thank: Duncan Muir for A-SEM related assistance; Tony Oldroyd for the timely production of high quality thin sections; the Grosvenor Estate for access to the Ben Strome field area; and Alan Hastie and Åke Fagereng, who provided helpful and encouraging comments on the thesis chapter that forms the basis of this paper. The manuscript also benefited from discussions with Kathryn Goodenough and Kate Abernethy. We would like to sincerely thank Tim Johnson and Hugh Rollinson, whose comments on a previous version of the manuscript greatly improved the clarity and quality of this paper. We would also like to thank Tim Johnson (again) and an anonymous reviewer, whose helpful comments helped to further improve this manuscript.

TABLES AND CAPTIONS

658 Table 1: Modal mineral proportions for the studied ultramafic rocks. Abbreviations: EM? = element
659 map?; ol = olivine; srp = serpentine; opx = orthopyroxene; cpx = clinopyroxene; amf = amphibole;
660 spn = spinel. *From Guice et al. (2018b). ^excludes vein samples.

Complex	Sample	Grid ref (NC)	EM?	ol	srp	opx	cpx	amf	spn
Achiltibuie	Lw16_799A	03048/07951	Y	8.8	0.0	19.0	36.9	34.4	1.0
Achiltibuie	Lw16_799B	03048/07951	Y	2.0	8.1	50.2	7.8	30.9	1.1
Achmelvich	Lw16-619B	05749/24184	Y	0.0	0.0	0.0	0.0	100.0	0.0
Achmelvich	Lw16-620A	05586/24174	Y	0.0	0.0	0.0	1.7	98.4	0.0
Achmelvich	LW17-Am2	05688/24284	Y	0.0	0.0	4.3	0.0	95.0	0.8
Ben Dreavie	LW17-BD1	26738/38805	Y	0.0	0.0	84.3	14.8	0.0	0.9
Ben Dreavie	LW17-BD2	26738/38805	Y	2.5	2.9	51.1	29.1	13.3	1.1
Drumbeg	LW17-Db3b	11067/33060	Y	0.0	32.4	30.8	9.0	26.5	1.4
Drumbeg	LW17-Db8	11255/33061	Y	2.0	18.6	7.9	0.0	70.4	1.2
Drumbeg	LW17-44	11472/33323	Y	0.0	5.2	52.1	13.7	28.7	0.4
Drumbeg	LW17-45A	11455/33353		1.5	0.5	52.0	5.0	39.0	2.0
Gorm Chnoc	LW17-GC2	21912/44749	Y	0.4	7.0	31.6	6.7	54.0	0.2
Gorm Chnoc	LW17-GC3	21912/44749		1.5	15.0	8.0	18.0	55.0	2.5
Gorm Chnoc	LW17-GC5	21954/44751	Y	4.7	28.1	2.8	0.0	64.4	0.0
Loch Eilean na Craoibhe Moire	Lw16_627B	21188/43446		0.0	0.0	39.8	10.0	50.0	0.2
Loch Eilean na Craoibhe Moire	Lw16_629B	21127/43493	Y	0.0	0.0	42.4	2.9	50.9	3.9
Loch Eilean na Craoibhe Moire	LW17-E1	21448/43096	Y	0.0	0.0	16.1	33.4	49.9	0.6
Loch Eilean na Craoibhe Moire	LW17-E2A	21448/43096	Y	0.0	9.3	38.0	6.4	46.4	0.0
Loch Eilean na Craoibhe Moire	LW17-E2B	21448/43096		4.5	1.0	25.0	45.0	23.0	1.5
Loch Eilean na Craoibhe Moire	LW17-E2C	21448/43096		15.5	26.0	40.0	12.0	4.0	2.5
Loch Eilean na Craoibhe Moire	LW17-E3	21448/43096	Y	0.0	19.1	42.8	6.9	31.2	0.0
Loch Eilean na Craoibhe Moire	LW17-E5	21448/43096	Y	4.0	10.2	48.0	8.3	28.3	1.2
Loch an Daimh Mor	UBCr_P1		Y	0.0	40.7	56.5	1.2	0.0	1.6
Loch an Daimh Mor	UBCr_P3		Y	0.0	37.5	42.2	6.7	12.5	1.2
Loch an Daimh Mor	X11A		Y	0.0	54.5	5.9	0.0	39.6	0.0
Loch an Daimh Mor	X11B			0.0	100.0	0.0	0.0	0.0	0.0
Loch an Daihm Mor - vein	UBZr_1a			0.0	25.0	60.0	5.0	10.0	0.0
Loch an Daihm Mor - vein	LEW014A	15621/41834	Y	0.0	0.0	97.1	0.2	2.7	0.0
North Scourie Bay	NSB_UMa			0.0	0.0	75.0	0.0	23.0	2.0
North Scourie Bay	NSB_UMb			3.5	0.0	31.0	31.0	33.0	1.5
Scourimore	T2190		Y	0.0	4.0	7.4	48.1	37.6	2.9
Scourimore	T2160L		Y	0.0	20.0	37.5	19.0	21.1	2.4
Scourimore	T2160U		y	0.0	18.9	45.7	26.6	7.1	1.7
Scourimore	T2110		Y	0.0	0.0	20.4	22.6	54.7	2.3
Scourimore	X3		Y	0.0	0.0	0.0	0.2	99.8	0.0
Scourimore	Lw16_643B	14230/44184	Y	19.0	0.0	40.5	18.4	21.0	1.0
Scourimore	Lw16_657	14209/44227	Y	0.0	0.0	28.8	23.8	44.8	2.6
Average				ol	srp	opx	cpx	amf	spn
<i>Ben Strome (n=33)*</i>				1	30	27	17	24	1
Achiltibuie (n=2)				5	4	35	22	33	1
Achmelvich (n=2)				0	0	0	1	99	0
Ben Dreavie (n=2)				1	1	68	22	7	1
Drumbeg (n=4)				1	14	36	7	41	1
Gorm Chnoc (n=3)				2	17	14	8	58	1
Loch Eilean na Craoibhe Moire (n=8)				3	8	37	16	35	1
Loch an Daimh Mor (n=4)^				0	58	26	2	13	1
North Scourie Bay (n=2)				2	0	53	16	28	2
Scourimore (n=7)				3	6	26	23	41	2
Range				ol	srp	opx	cpx	amf	spn
<i>Ben Strome</i>				< 5	< 100	< 91	< 45	< 78	< 5
Achiltibuie				2 - 9	< 8	19 - 50	8 - 37	31 - 35	1
Achmelvich				0	0	< 4.3	< 1.7	> 95	< 1
Ben Dreavie				< 2.5	< 3	51 - 84	15 - 30	< 13	1
Drumbeg				< 2	< 32	8 - 52	< 14	27 - 70	< 2
Gorm Chnoc				< 5	7 - 28	3 - 32	< 18	54 - 64	< 2.5
Loch Eilean na Craoibhe Moire				< 16	26	16 - 48	3 - 45	4 - 51	< 4
Loch an Daimh Mor				0	> 38	< 57	< 7	< 40	< 2
North Scourie Bay				< 3.5	0	31 - 75	< 31	23 - 33	1.5 - 2
Scourimore				< 19	< 20	< 46	< 48	> 7	< 3

661

662 Table 2: Modal mineral proportions for the studied mafic rocks. Abbreviations: EM? = element map?;
663 opx = orthopyroxene; cpx = clinopyroxene; amf = amphibole; fel = feldspar; gnt = garnet; qtz = quartz;
664 ox = oxide minerals.

Complex	Sample	Grid ref (NC)	EM?	opx	cpx	amf	fel	gnt	qtz	ox
Ben Auskaird	LEW004	20926/40272		0.0	0.0	84.0	13.0	0.0	3.0	0.0
Ben Strome	LEW010	25375/35591		2.0	8.0	71.0	2.0	12.0	0.0	5.0
Ben Strome	LEW011	25716/36120		16.0	16.0	12.0	13.0	35.0	0.0	8.0
Ben Strome	LEW012	25553/36005		30.0	60.0	10.0	0.0	0.0	0.0	0.0
Ben Strome	Lw16_510b	24879/35626		8.0	22.0	11.0	27.0	32.0	0.0	0.0
Ben Strome	Lw16_Z2a-1	26067/35391		2.0	7.0	46.0	24.5	18.0	0.5	2.0
Ben Strome	Lw16_Z2a-2	26067/35391		0.0	0.0	65.0	35.0	0.0	0.0	0.0
Ben Strome	Lw16_Z2b	26067/35391		5.0	30.0	65.0	0.0	0.0	0.0	0.0
Ben Strome	Lw16_Z13b	26073/35578	Y	0.0	2.7	51.9	45.0	0.0	0.4	0.0
Ben Strome	Lw16_Z13c	26073/35578	Y	0.0	35.8	39.9	15.4	7.9	1.0	0.0
Ben Strome	Lw16_Z14a	26073/35585		9.0	48.0	23.0	8.0	12.0	0.0	0.0
Ben Strome	Lw16_Z14b	26073/35585		0.0	4.8	75.0	20.0	0.0	0.2	0.0
Ben Strome	Lw16_Z15	26077/35593		0.0	49.0	20.0	18.0	11.0	0.0	2.0
Geodh' nan Sgadan	LW17-BcT3	14632/41779	Y	11.2	0.0	82.3	6.5	0.0	0.0	0.0
Geodh' nan Sgadan	LW17-BcT4	14631/41780		5.0	6.0	44.0	45.0	0.0	0.0	0.0
Geodh' nan Sgadan	LW17-BcT6	14628/41784	Y	0.0	27.9	71.5	0.0	0.0	0.6	0.0
Geodh' nan Sgadan	LW17-BcT8	14627/41801	Y	0.0	35.4	0.0	64.1	0.0	0.0	0.5
Geodh' nan Sgadan	LW17-BcT12A	14625/41836		0.0	0.0	20.0	66.0	14.0	0.0	0.0
Gorm Chnoc	LW17-GC1	22139/44569		0.0	0.0	85.0	15.0	0.0	0.0	0.0
Gorm Chnoc	LW17-GC4	22156/44613		0.0	0.0	70.0	30.0	0.0	0.0	0.0
Average				opx	cpx	amf	fel	gnt	qtz	ox
<i>Ben Strome (n=12)</i>				6	24	41	17	11	0	1
<i>Ben Auskaird (n=1)</i>				0	0	84	13	0	3	0
<i>Gorm Chnoc (n=2)</i>				0	0	78	23	0	0	0
<i>Geodh' nan Sgadan (n=5)</i>				3	14	44	36	3	0	0
Range				opx	cpx	amf	fel	gnt	qtz	ox
<i>Ben Strome (n=12)</i>				< 30	< 60	10 - 75	< 45	< 35	< 1	< 8
<i>Ben Auskaird (n=1)</i>				0	0	84	13	0	3	0
<i>Gorm Chnoc (n=2)</i>				0	0	70 - 85	15 - 30	0	0	0
<i>Geodh' nan Sgadan (n=5)</i>				< 11	< 35	< 82	< 66	< 14	< 1	< 1

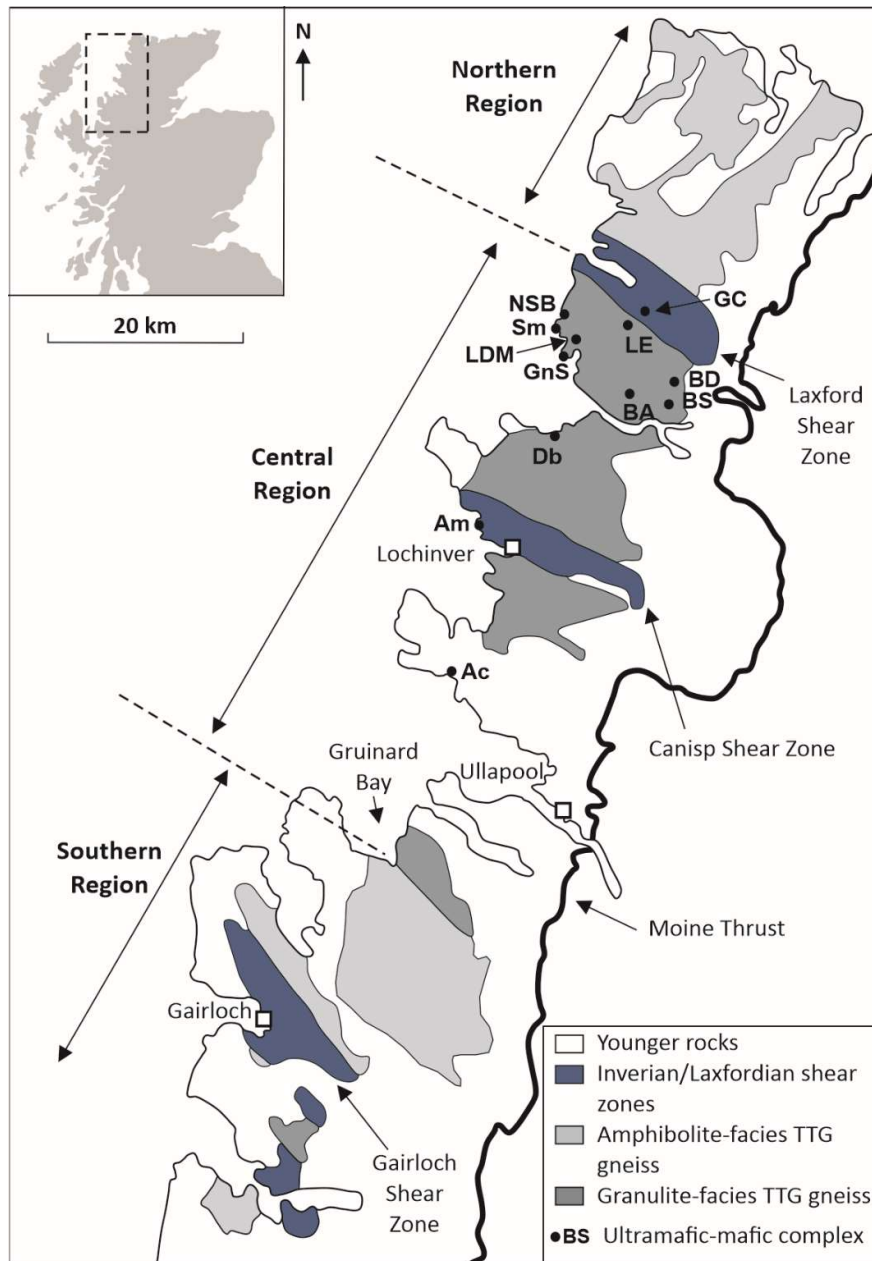
665

666

667 Table 3: Major, minor, trace and platinum-group element characteristics of the 12 ultramafic-mafic complexes, alongside a comparison between Ben Strome
668 and each complex studied here Abbreviations: LDM = Loch an Daimh Mor; LEC = Loch Eilean na Craoibhe Moire; NSB = North Scourie Bay; GnS = Geodh' nan
669 Sgadan; chonN = chondrite normalised; pmN = primitive mantle normalised; PGE = platinum-group elements. *major, minor and trace elements are from
670 Guice et al. (2018b). PGE are from this study. ^ trace elements are those considered by Guice et al. (2018b) to most closely resemble primary magmatic
671 compositions. Other symbols: tick = comparable to the Ben Strome Complex; cross = distinct from the Ben Strome Complex; backwards slash = relatively
672 minor, but notable distinction. Underlined cross = feature can likely be explained by secondary processes.

Locality Unit	n=	Major and minor elements (Fig. 5)							Trace elements (Figs. 6-7)				PGE (Fig. 8)	
		MgO wt. %	SiO ₂ wt. %	TiO ₂ wt. %	Al ₂ O ₃ wt. %	CaO wt. %	Cr ₂ O ₃ wt. %	NiO wt. %	La/Lu chonN	La/Sm chonN	Nb/Yb pmN	La/Ta pmN	Pd/Ir chonN	Total PGE ppb
Ultramafic rocks														
Ben Strome*^	35	18 - 48	36 - 48	0.1 – 0.7	2 - 13	1 - 12	0.1 - 0.5	0.1 - 1	0.5 - 2	0.6 - 2.2	0.4 - 3.9	0.3 - 2.0	2 - 33	5 – 34
Achmelvich	4	17 - 28	45 - 50	0.3 – 0.4	6 – 8	7 - 10	0.3 - 0.5	0.1 - 0.8	0.4 - 0.6	0.3 - 0.5	0.4 - 2.5	0.6 - 0.8	6 - 11	9 – 11
Achiltibuie	3	27 - 31	45 - 57	0.2 – 0.3	4 – 6	6 - 8	0.4	0.1 - 0.3	0.7 - 2.3	0.6 - 1.9	0.8 - 2.6	0.2 - 0.9	5 - 9	15 - 24
Ben Dreavie	2	27 - 29	47 - 49	0.2 – 0.3	5	3 - 6	0.4	0.1 - 0.2	15 - 20	6.1 - 9.7	0.5 - 1.6	5.8 - 31.5	3 - 8	33 – 39
Drumbeg	9	21 - 32	43 - 47	0.2 – 0.6	4 – 11	5 - 9	0.1 - 0.4	0.1 - 0.2	0.6 - 1.9	0.5 - 1.3	0.6 - 1.2	0.6 - 1.7	7 - 16	14 – 75
Gorm Chnoc	3	25 - 28	40 - 46	0.2 – 0.3	7 - 10	5 - 7	< 0.4	0.1	1.8 - 2.1	0.6 - 2.1	0.5 - 0.6	2.8 - 3.2	117 - 124	18 – 24
LDM	5	35 - 42	46 - 51	< 0.2	2 - 4	< 1.5	0.1 - 0.4	0.3 - 0.4	0.2 - 8.4	1.5 - 3.2	0.5 - 2.2	0.2 - 9.0	0.2 - 4	3 – 30
LEC	9	26 - 40	40 - 49	0.1 – 0.4	3 – 8	1 - 8	0.3 - 0.7	0.1 - 0.6	1.0 - 2.9	0.9 - 2.9	0.4 - 2.9	0.8 - 2.0	2 - 13	11 – 45
NSB	1	21	48	0.4	7	10	0.3	0.1	2.7	1.5	1.2	1.7	10	22
Scouriemore	9	19 - 31	43 - 48	0.2 – 0.5	5 – 9	6 - 14	0.3 - 0.5	0.1 - 0.2	0.8 - 5.0	0.7 - 2.2	0.6 - 2.2	0.7 - 1.7	2 - 25	13 - 34
Mafic rocks														
Ben Strome	17	5 - 21	39 - 49	0.3 – 16	8 – 17	9 - 17	< 0.2	< 0.1	0.3 - 8	0.2 - 3.1	0.3 - 1.9	< 8.8	24 - 46	1 - 6
Ben Auskaird	2	3 - 4	48 - 60	3	13	7 - 8	< 0.1	< 0.1	2.0 - 3.1	1.3 - 2.5	2.2	0.8 - 1.5	18 - 44	3 - 18
Drumbeg	1	10	49	0.9	14	11	< 0.1	< 0.1	7	1.5	0.8	8.2	n/a	n/a
GnS	5	5 - 14	45 - 54	0.2 – 1.6	14 – 20	9 - 13	< 0.3	< 0.1	2.0 - 4.7	1.7 - 2.8	0.5 - 1.5	1.6 - 8	8 - 24	11 – 12
Gorm Chnoc	2	12 - 14	48 - 49	0.2	14 – 15	14	< 0.2	< 0.1	0.6 - 0.9	0.6 - 0.8	0.2 - 0.3	2.0 - 5.2	n/a	n/a

673



675

676 Figure 1: Simplified geological map of the LGC detailing the locations of the ultramafic-mafic
 677 complexes investigated as part of this study (redrawn after: Johnson et al., 2012; Kinny et al., 2005;
 678 Wheeler et al., 2010). Abbreviations: Ac=Achiltibuie; Am=Achmelvich; BA=Ben Auskaird; BD=Ben
 679 Dreavie; BS=Ben Strome; Db=Drumbeg; GC=Gorm Chnoc; GnS=Geodh' nan Sgadan; LDM=Loch an
 680 Daimh Mor; LE=Loch Eilean na Craoibhe Moire; NSB=North Scourie Bay; Sm=Scouriemore.

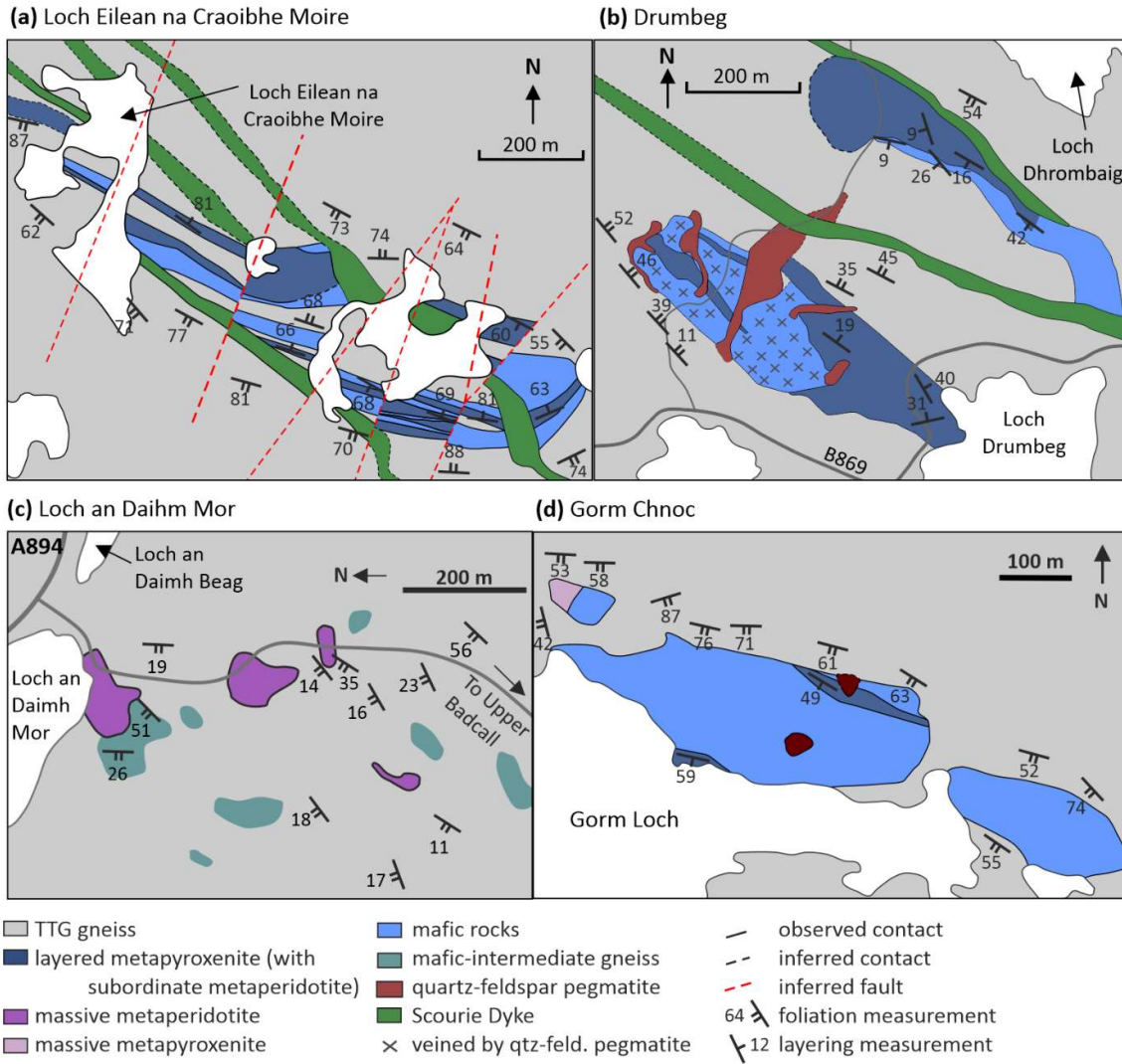
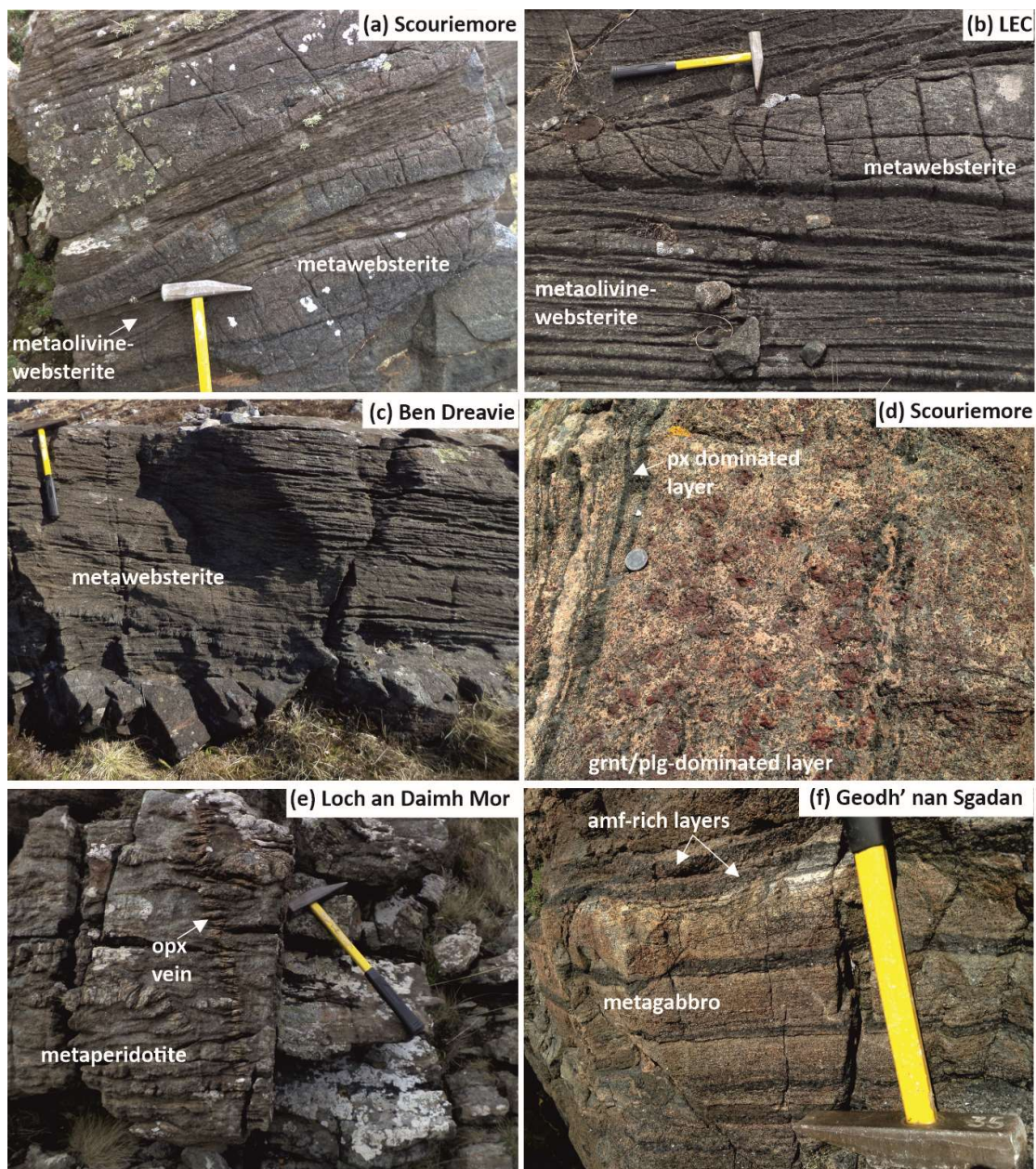
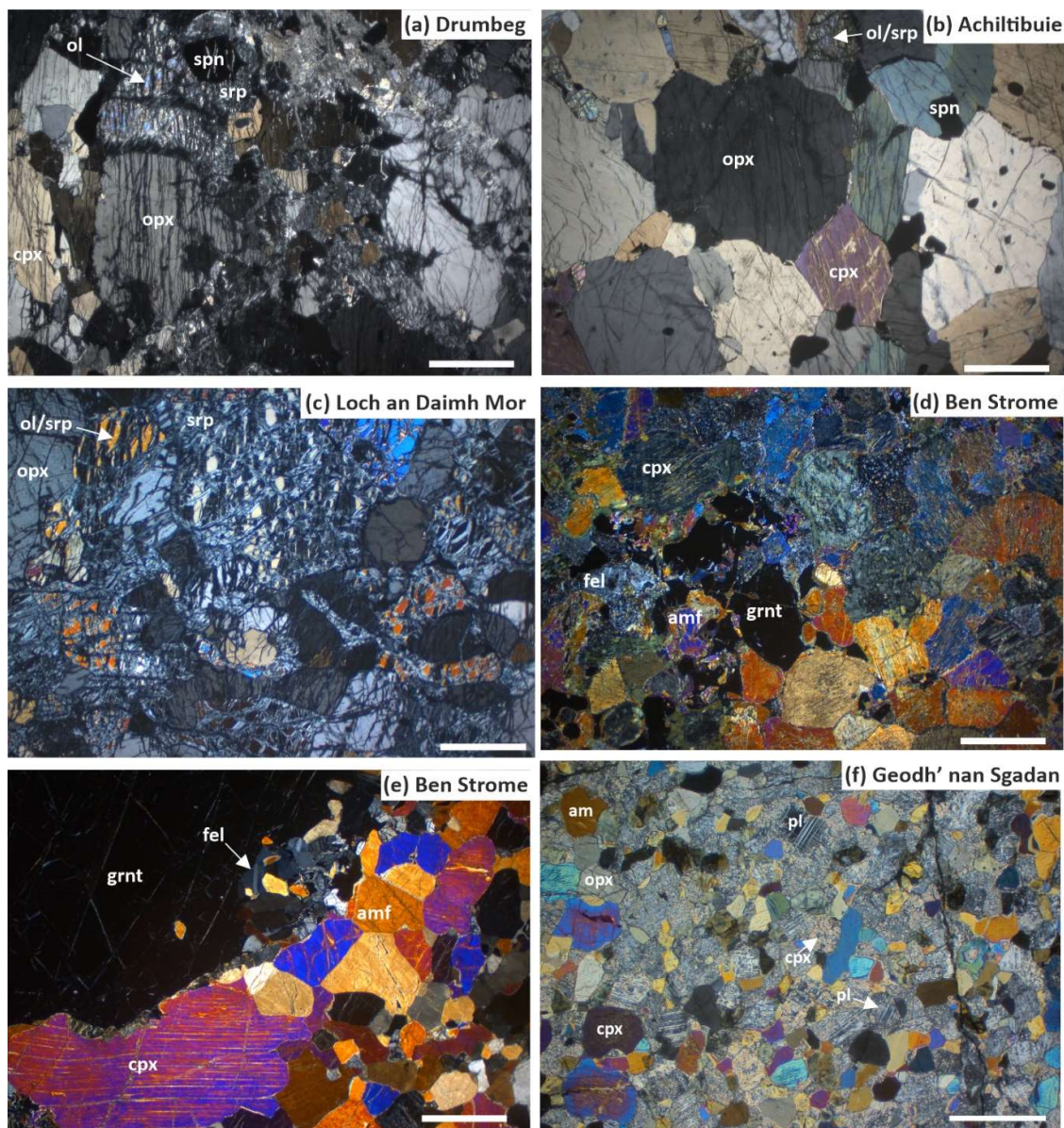


Figure 2: Simplified geological maps of the Loch Eilean na Craoibhe Moire, Drumbeg, Loch an Daimh Mor and Gnoc Gorm Complexes. The location of each complex is detailed in Figure 1.



684

685 Figure 3: Field photographs detailing the representative rock types that comprise the ultramafic-mafic
 686 complexes studied.



687

688 Figure 4: Photomicrographs (XPL) detailing the petrographic characteristics of the studied rocks. White
 689 scale bar = 1 mm.

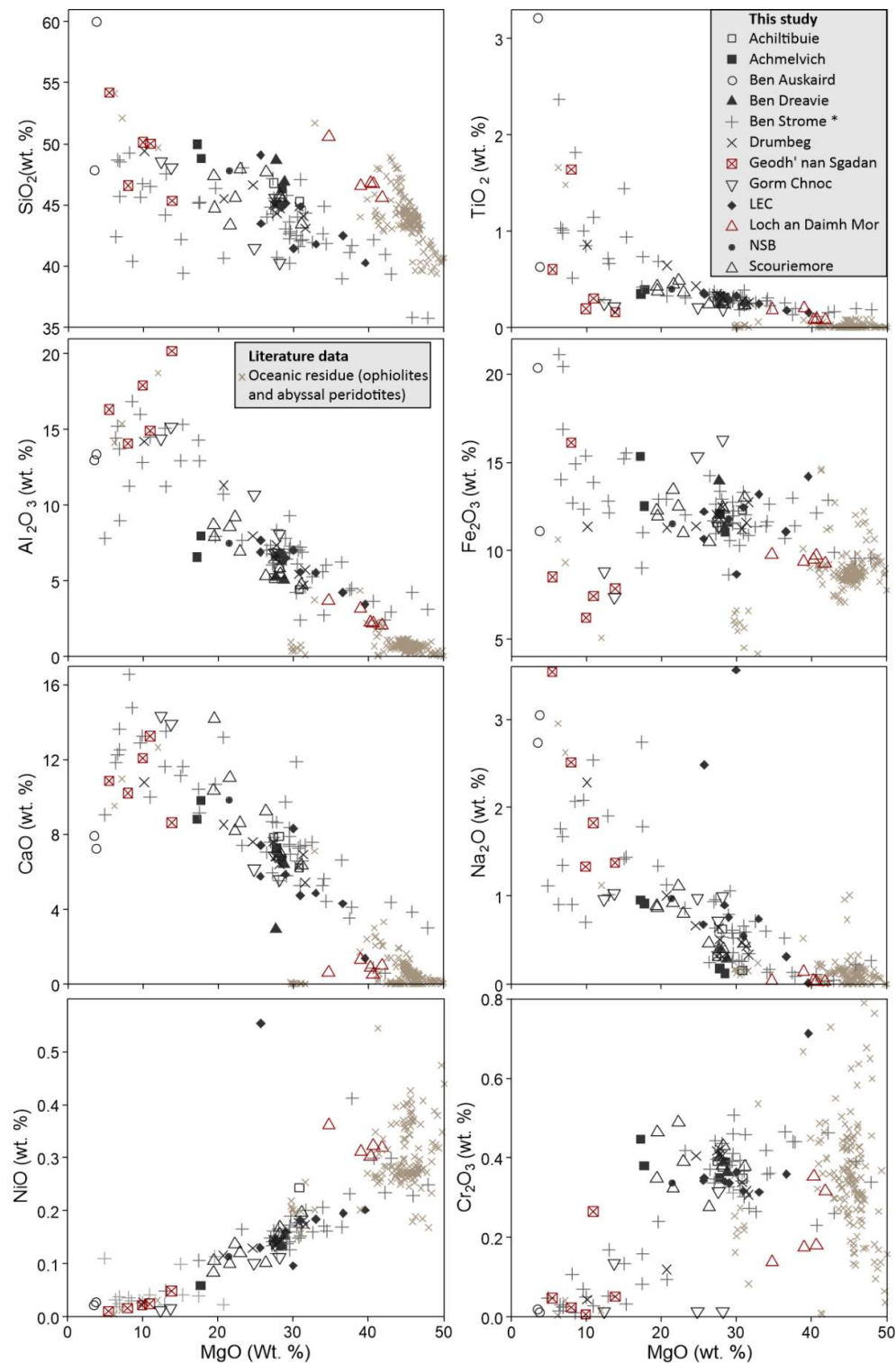
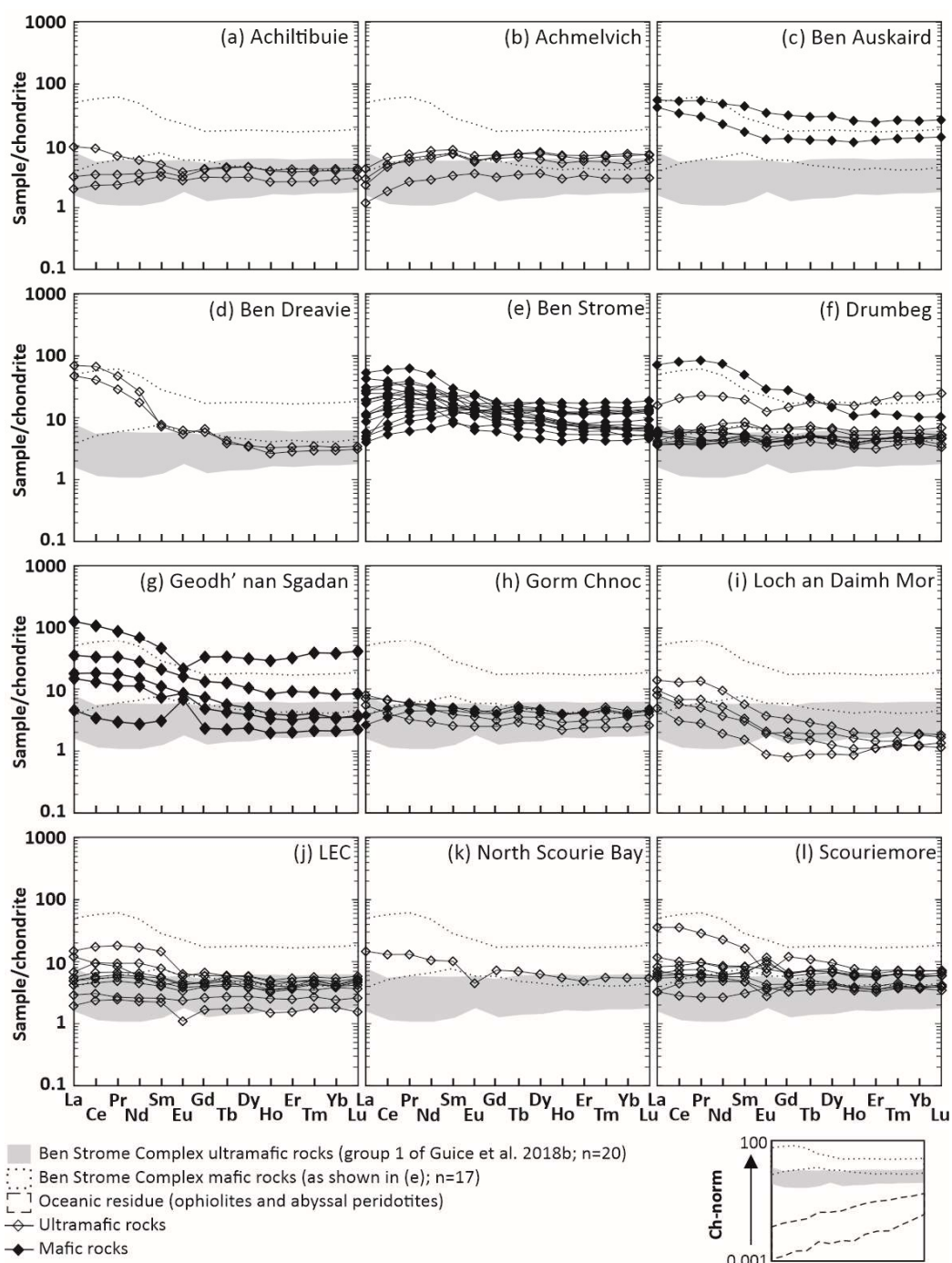
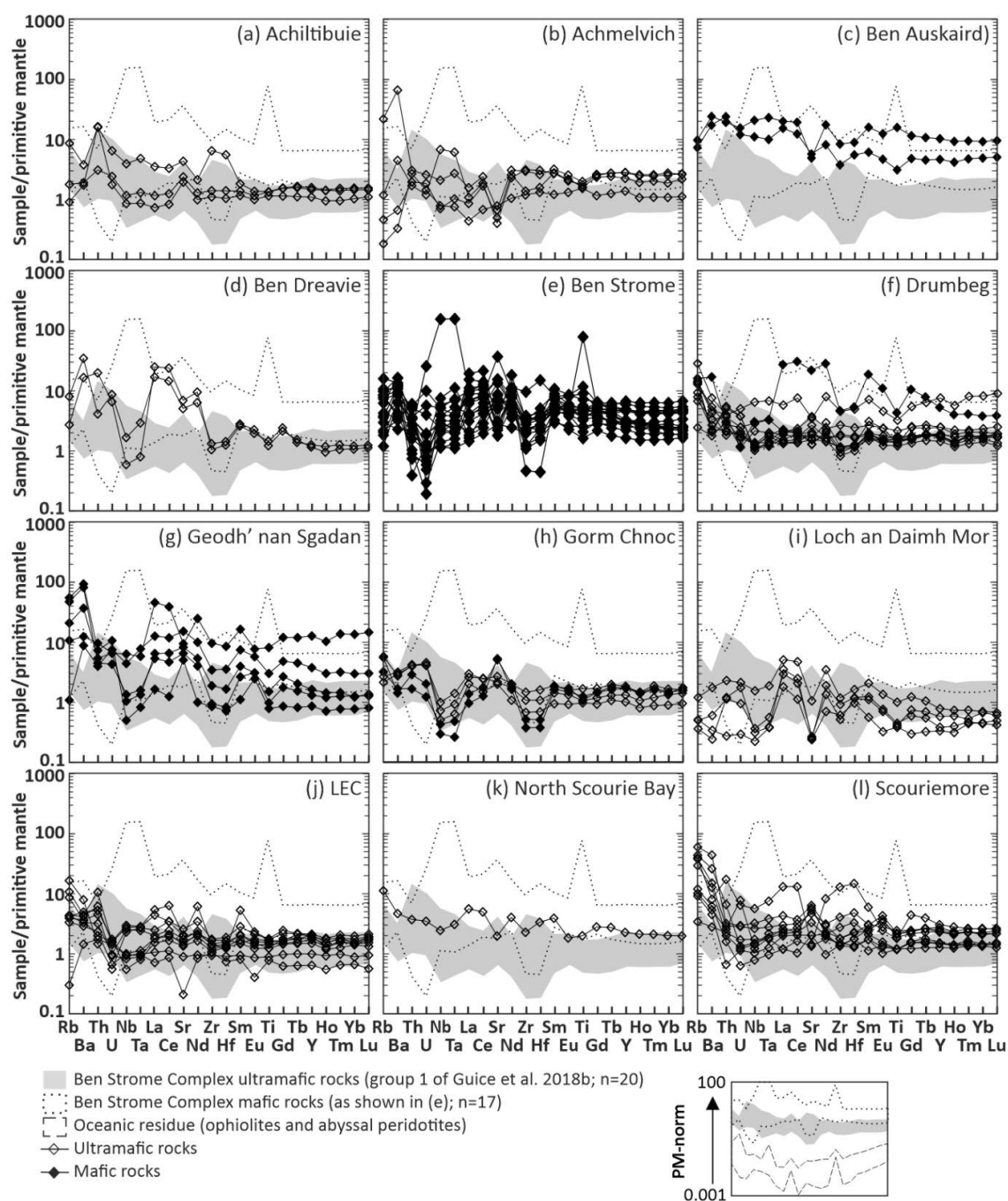


Figure 5: Bivariate plots detailing the anhydrous major and minor-element compositions of the ultramafic-mafic rocks analysed from the 12 studied complexes. *Ben Strome data includes 35 ultramafic samples published in Guice et al. (2018b).



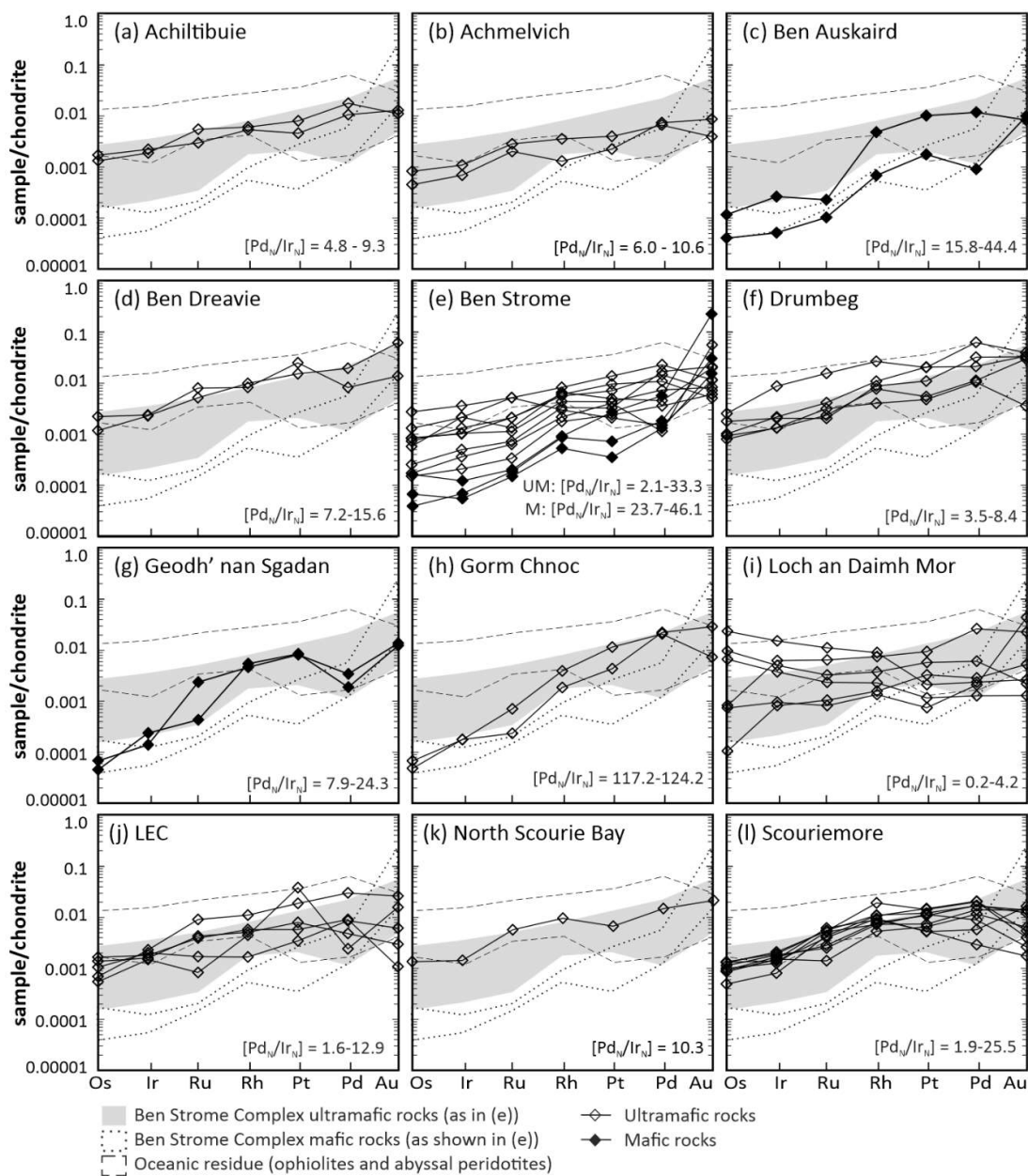
694

695 Figure 6: Chondrite-normalised (McDonough and Sun, 1995) REE plots for the analysed ultramafic-
696 mafic rocks from the 12 studied complexes.



697

698 Figure 7: Primitive mantle-normalised (McDonough and Sun, 1995) trace element plots for the
 699 analysed ultramafic-mafic rocks from the 12 studied complexes.



700

701 Figure 8: Chondrite-normalised (Lodders, 2003) PGE (+Au) plots for the analysed ultramafic-mafic
 702 rocks from the 12 studied complexes. Abbreviations: UM = ultramafic; M = mafic.

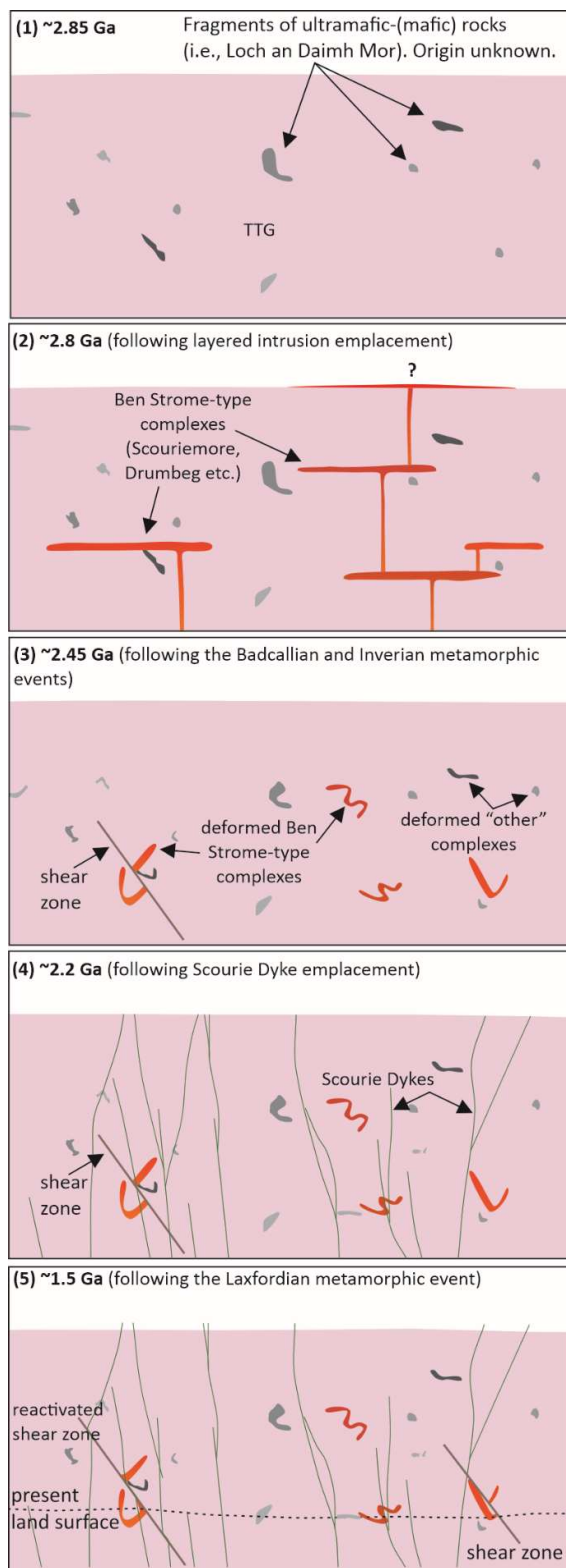


Figure 9: Schematic diagram detailing the proposed evolution of the LGC.

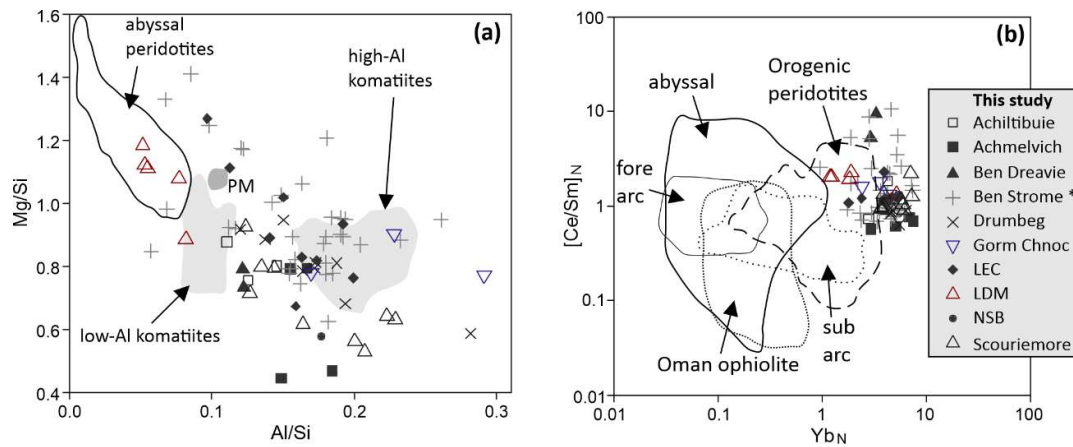


Figure 10: (a) Mg/Si versus Al/Si (wt. %) plot for the ultramafic rocks analysed as part of this study. (b) Chondrite-normalised [Ce/Yb] versus [Yb] plot for the ultramafic rocks analysed as part of this study. Fields are after: Rollinson (2007). Abbreviations: PM = primitive mantle. LEC = Loch Eilean na Craoibhe Moire LDM = Loch an Daimh Mor; NSB = North Scourie Bay. * = includes ultramafic samples published by Guice et al. (2018b).

REFERENCES

- Andersen, T., Whitehouse, M.J., Burke, E.A.J., 1997. Fluid inclusions in Scourian granulites from the Lewisian complex of NW Scotland: evidence for CO₂-rich fluid in Late Archaean high-grade metamorphism. *Lithos* 40, 93–104.
- Arndt, N.T., 2013. Formation and Evolution of the Continental Crust. *Geochemical Perspect.* 2, 405–533. <https://doi.org/10.7185/geochempersp.2.3>
- Barnes, S.J., Naldrett, A.J., Gorton, M.P., 1985. The origin of the fractionation of platinum-group elements in terrestrial magmas. *Chem. Geol.* 53, 303–323. [https://doi.org/10.1016/0009-2541\(85\)90076-2](https://doi.org/10.1016/0009-2541(85)90076-2)
- Barnicoat, A.C., 1983. Metamorphism of the Scourian Complex, NW Scotland. *J. Metamorph. Geol.* 1,

722 163–182.

723 Barnicoat, A.C., O'Hara, M.J., 1978. High-temperature pyroxenes from an ironstone at Scourie,
 724 Sutherland. *Mineral. Mag.* 43, 371–375.

725 Barooah, B.C., Bowes, D.R., 2009. Multi-episodic modification of high-grade terrane near Scourie and
 726 its significance in elucidating the history of the Lewisian Complex. *Scottish J. Geol.* 45, 19–41.
 727 <https://doi.org/10.1144/0036-9276/01-384>

728 Beach, A., 1974. Amphibolitization of Scourian granulites. *Scottish J. Geol.* 10, 35–43.

729 Beach, A., 1973. The mineralogy of high temperature shear zones at Scourie, N.W. Scotland. *J.*
 730 *Petrol.* 14, 231–248.

731 Beach, A., Coward, M.P., Graham, R.H., 1974. An interpretation of the structural evolution of the
 732 Laxford Front, north-west Scotland. *Scottish J. Geol.* 9, 297–308.

733 Bédard, J.H., 2018. Stagnant lids and mantle overturns : Implications for Archaean tectonics ,
 734 magmagenesis , crustal growth , mantle evolution , and the start of plate tectonics. *Geosci.*
 735 *Front.* 9, 19–49. <https://doi.org/10.1016/j.gsf.2017.01.005>

736 Bédard, J.H., Harris, L.B., Thurston, P.C., 2013. The hunting of the snArc. *Precambrian Res.* 229, 20–
 737 48. <https://doi.org/10.1016/j.precamres.2012.04.001>

738 Bowen, N.L., 1956. The evolution of igneous rocks. Dover Publications, New York.

739 Bowes, D.R., Park, R.G., Wright, A.E., 1964. Layered intrusive rocks in the Lewisian of the North-West
 740 Highlands of Scotland. *Q. J. Geol. Soc.* 120, 153. <https://doi.org/10.1144/gsjgs.120.1.0153>

741 Brown, M., Johnson, T.E., 2018. Secular change in metamorphism and the onset of global plate
 742 tectonics. *Am. Mineral.* 103, 181–196. <https://doi.org/10.2138/am-2018-6166>

743 Burton, K.W., Capmas, F., Birck, J.L., Allegre, C.J., Cohen, A.S., 2000. Resolving crystallisation ages of
 744 Archean mafic-ultramafic rocks using the Re-Os isotope system. *Earth Planet. Sci. Lett.* 179,

745 453–467.

746 Cartwright, I., Fitches, W.R., O’Hara, M.J., Barnicoat, A.C., O’Hara, S., 1985. Archaean supracrustal
 747 rocks from the Lewisian near Stoer, Sutherland. *Scottish J. ...* 21, 187–196.
 748 <https://doi.org/10.1144/sjg21020187>

749 Cawood, P.A., Hawkesworth, C.J., Pisarevsky, S.A., Dhuime, B., Capitanio, F.A., Nebel, O., 2018.
 750 Geological archive of the onset of plate tectonics. *Phil. Trans. R. Soc. Lond.* 376.

751 Condie, K.C., 2018. A planet in transition: The onset of plate tectonics on Earth between 3 and 2 Ga?
 752 *Geosci. Front.* 9, 51–60. <https://doi.org/10.1016/j.gsf.2016.09.001>

753 Corfu, F., 1998. U-Pb zircon systematics at Gruinard Bay, northwest Scotland : implications for the
 754 early orogenic evolution of the Lewisian complex. *Contrib. to Mineral. Petrol.* 133, 329–345.

755 Corfu, F., Heaman, L.M., Rogers, G., 1994. Polymetamorphic evolution of the Lewisian complex, NW
 756 Scotland, as recorded by U-Pb isotopic compositions of zircon, titanite and rutile. *Contrib. to*
 757 *Mineral. Petrol.* 117, 215–228.

758 Crowley, Q.G., Key, R., Noble, S.R., 2015. High-precision U–Pb dating of complex zircon from the
 759 Lewisian Gneiss Complex of Scotland using an incremental CA-ID-TIMS approach. *Gondwana*
 760 *Res.* 27, 1381–1391. <https://doi.org/10.1016/j.gr.2014.04.001>

761 Davies, J.H.F.L., Heaman, L.M., 2014. New U-Pb baddeleyite and zircon ages for the Scourie dyke
 762 swarm: A long-lived large igneous province with implications for the Paleoproterozoic evolution
 763 of NW Scotland. *Precambrian Res.* 249, 180–198.
 764 <https://doi.org/10.1016/j.precamres.2014.05.007>

765 Dhuime, B., Wuestefeld, A., Hawkesworth, C.J., 2015. Emergence of modern continental crust about
 766 3 billion years ago. *Nat. Geosci.* 8, 552–555. <https://doi.org/10.1038/NGEO2466>

767 Evans, C.R., Lambert, R.S.J., 1974. The Lewisian of Lochinver, Sutherland; the type area for the

768 Inverian metamorphism. *J. Geol. Soc. London.* 130, 125–150.
 769 <https://doi.org/10.1144/gsjgs.130.2.0125>

770 Faithfull, J.W., Dempster, T.J., MacDonald, J.M., Reilly, M., 2018. Metasomatism and the
 771 crystallization of zircon megacrysts in Archaean peridotites from the Lewisian complex, NW
 772 Scotland. *Contrib. to Mineral. Petrol.* 173, 99. <https://doi.org/10.1007/s00410-018-1527-5>

773 Feisel, Y., White, R.W., Palin, R.M., Johnson, T.E., 2018. New constraints on granulite facies
 774 metamorphism and melt production in the Lewisian Complex, northwest Scotland. *J.*
 775 *Metamorph. Geol.* 1–21. <https://doi.org/10.1111/jmg.12311>

776 Friend, C.R.L., Kinny, P.D., 2001. A reappraisal of the Lewisian Gneiss Complex: geochronological
 777 evidence for its tectonic assembly from disparate terranes in the Proterozoic. *Contrib. to*
 778 *Mineral. Petrol.* 142, 198–218. <https://doi.org/10.1007/s004100100283>

779 Furnes, H., Robins, B., De Wit, M.J., 2012. Geochemistry and petrology of lavas in the upper
 780 onverwacht suite, Barberton Mountain Land, South Africa. *South African J. Geol.* 115, 171–210.
 781 <https://doi.org/10.2113/gssajg.115.2.171>

782 Godard, M., Jousset, D., Bodinier, J., 2000. Relationships between geochemistry and structure
 783 beneath a palaeo-spreading centre: a study of the mantle section in the Oman ophiolite. *Earth*
 784 *Planet. Sci. Lett.* 180, 133–148.

785 Godard, M., Lagabriele, Y., Alard, O., Harvey, J., 2008. Geochemistry of the highly depleted
 786 peridotites drilled at ODP Sites 1272 and 1274 (Fifteen-Twenty Fracture Zone, Mid-Atlantic
 787 Ridge): Implications for mantle dynamics beneath a slow spreading ridge. *Earth Planet. Sci.*
 788 *Lett.* 267, 410–425. <https://doi.org/10.1016/j.epsl.2007.11.058>

789 Goodenough, K.M., Crowley, Q.G., Krabbendam, M., Parry, S.F., 2013. New u–pb age constraints for
 790 the Laxford Shear Zone, NW Scotland: Evidence for tectono-magmatic processes associated
 791 with the formation of a paleoproterozoic supercontinent. *Precambrian Res.* 232, 1–19.

792 <https://doi.org/10.1016/j.precamres.2013.05.006>

793 Goodenough, K.M., Park, R.G., Krabbendam, M., Myers, J.S., Wheeler, J., Loughlin, S.C., Crowley,
794 Q.G., Friend, C.R.L., Beach, A., Kinny, P.D., Graham, R.H., 2010. The Laxford Shear Zone: an end-
795 Archaean terrane boundary? *Geol. Soc. London, Spec. Publ.* 335, 103–120.
796 <https://doi.org/10.1144/SP335.6>

797 Guice, G.L., 2019. Origin and geodynamic significance of ultramafic-mafic complexes in the North
798 Atlantic and Kaapvaal Cratons. Cardiff University.

799 Guice, G.L., McDonald, I., Hughes, H.S.R., Anhaeusser, C.R., 2019. An evaluation of element mobility
800 in the Modderfontein ultramafic complex, Johannesburg: Origin as an Archaean ophiolite
801 fragment or greenstone belt remnant? *Lithos* 332–333, 99–119.
802 <https://doi.org/10.1016/j.lithos.2019.02.013>

803 Guice, G.L., McDonald, I., Hughes, H.S.R., MacDonald, J.M., Blenkinsop, T.G., Goodenough, K.M.,
804 Faithfull, J.W., Gooday, R.J., 2018a. Re-evaluating ambiguous age relationships in Archean
805 cratons: Implications for the origin of ultramafic-mafic complexes in the Lewisian Gneiss
806 Complex. *Precambrian Res.* 311, 136–156. <https://doi.org/10.1016/j.precamres.2018.04.020>

807 Guice, G.L., McDonald, I., Hughes, H.S.R., Schlatter, D.M., Goodenough, K.M., Macdonald, J.M.,
808 Faithfull, J.W., 2018b. Assessing the Validity of Negative High Field Strength-Element Anomalies
809 as a Proxy for Archaean Subduction: Evidence from the Ben Strome Complex, NW Scotland.
810 *Geosciences* 8, 338. <https://doi.org/10.3390/geosciences8090338>

811 Halla, J., 2018. Highlights on Geochemical Changes in Archaean Granitoids and Their Implications for
812 Early Earth Geodynamics. *Geosciences* 8, 353. <https://doi.org/10.3390/geosciences8090353>

813 Heaman, L.M., Tarney, J., 1989. U–Pb Baddeleyite ages for the Scourie Dyke Swarm, Scotland –
814 evidence for 2 distinct intrusion events. *Nature* 340, 705–708.

815 Huber, H., Koeberl, C., McDonald, I., Reimold, W.U., 2001. Geochemistry and petrology of

816 Witwatersrand and dwyka diamictites from south Africa: Search for an extraterrestrial
 817 component. *Geochim. Cosmochim. Acta* 65, 2007–2016. [https://doi.org/10.1016/S0016-](https://doi.org/10.1016/S0016-7037(01)00569-5)
 818 [7037\(01\)00569-5](https://doi.org/10.1016/S0016-7037(01)00569-5)

819 Johnson, T.E., Brown, M., Gardiner, N.J., Kirkland, C.L., Smithies, R.H., 2017. Earth’s first stable
 820 continents did not form by subduction. *Nature*. <https://doi.org/10.1038/nature21383>

821 Johnson, T.E., Brown, M., Goodenough, K.M., Clark, C., Kinny, P.D., White, R.W., 2016. Subduction or
 822 sagduction ? Ambiguity in constraining the origin of ultramafic – mafic bodies in the Archean
 823 crust of NW Scotland. *Precambrian Res.* 283, 89–105.
 824 <https://doi.org/10.1016/j.precamres.2016.07.013>

825 Johnson, T.E., Fischer, S., White, R.W., 2013. Field and petrographic evidence for partial melting of
 826 TTG gneisses from the central region of the mainland Lewisian complex, NW Scotland. *J. Geol.*
 827 *Soc. London.* 170, 319–326. <https://doi.org/10.1144/jgs2012-096>

828 Johnson, T.E., Fischer, S., White, R.W., Brown, M., Rollinson, H.R., 2012. Archaean intracrustal
 829 differentiation from partial melting of metagabbro-field and geochemical evidence from the
 830 central region of the Lewisian complex, NW Scotland. *J. Petrol.* 53, 2115–2138.
 831 <https://doi.org/10.1093/petrology/egs046>

832 Johnson, T.E., Kirkland, C.L., Gardiner, N.J., Brown, M., Smithies, R.H., Santosh, M., 2019. Secular
 833 change in TTG compositions: Implications for the evolution of Archaean geodynamics. *Earth*
 834 *Planet. Sci. Lett.* 505, 65–75. <https://doi.org/10.1016/j.epsl.2018.10.022>

835 Kamber, B.S., 2015. The evolving nature of terrestrial crust from the Hadean, through the Archaean,
 836 into the Proterozoic. *Precambrian Res.* 258, 48–82.
 837 <https://doi.org/10.1016/j.precamres.2014.12.007>

838 Kinny, P., Friend, C., Love, G., 2005. Proposal for a terrane-based nomenclature for the Lewisian
 839 Gneiss Complex of NW Scotland. *J. Geol. Soc. London.* 162, 175–186.

840 <https://doi.org/10.1144/0016-764903-149>

841 Kinny, P.D., Friend, C.R.L., 1997. U-Pb isotopic evidence for the accretion of different crustal blocks
842 to form the Lewisian Complex of northwest Scotland. *Contrib. to Mineral. Petrol.* 129, 326–340.
843 <https://doi.org/10.1007/s004100050340>

844 Lodders, K., 2003. Solar System Abundances and Condensation Temperatures of the Elements.
845 *Astrophys. J.* 591, 1220–1247. <https://doi.org/10.1086/375492>

846 Love, G.J., Friend, C.R.L., Kinny, P.D., 2010. Palaeoproterozoic terrane assembly in the Lewisian
847 Gneiss Complex on the Scottish mainland, south of Gruinard Bay: SHRIMP U-Pb zircon
848 evidence. *Precambrian Res.* 183, 89–111. <https://doi.org/10.1016/j.precamres.2010.07.014>

849 Love, G.J., Kinny, P.D., Friend, C.R.L., 2004. Timing of magmatism and metamorphism in the Gruinard
850 Bay area of the Lewisian Gneiss Complex: Comparisons with the Assynt Terrane and
851 implications for terrane accretion. *Contrib. to Mineral. Petrol.* 146, 620–636.
852 <https://doi.org/10.1007/s00410-003-0519-1>

853 MacDonald, J.M., Goodenough, K.M., Wheeler, J., Crowley, Q., Harley, S.L., Mariani, E., Tatham, D.,
854 2015. Temperature-time evolution of the Assynt Terrane of the Lewisian Gneiss Complex of
855 Northwest Scotland from zircon U-Pb dating and Ti thermometry. *Precambrian Res.* 260, 55–
856 75. <https://doi.org/10.1016/j.precamres.2015.01.009>

857 McDonald, I., Viljoen, K.S., 2006. Platinum-group element geochemistry of mantle eclogites: a
858 reconnaissance study of xenoliths from the Orapa kimberlite, Botswana. *Appl. Earth Sci.* 115,
859 81–93. <https://doi.org/10.1179/174327506X138904>

860 McDonough, W.F., Sun, S. s., 1995. The composition of the Earth. *Chem. Geol.* 120, 223–253.
861 [https://doi.org/10.1016/0009-2541\(94\)00140-4](https://doi.org/10.1016/0009-2541(94)00140-4)

862 Moyen, J., Laurent, O., 2018. Archaean tectonic systems : A view from igneous rocks. *Lithos* 302–
863 303, 99–125. <https://doi.org/10.1016/j.lithos.2017.11.038>

- 864 Park, R.G., 2005. The Lewisian terrane model: a review. *Scottish J. Geol.* 41, 105–118.
865 <https://doi.org/10.1144/sjg41020105>
- 866 Park, R.G., Stewart, A.D., Wright, A.E., 2002. The Hebridean Terrane, in: *The Geology of Scotland*.
- 867 Park, R.G., Tarney, J., 1987. The Lewisian complex: a typical Precambrian high-grade terrain? *Geol.*
868 *Soc. London, Spec. Publ.* 27, 13–25. <https://doi.org/10.1144/gsl.sp.1987.027.01.03>
- 869 Paulick, H., Bach, W., Godard, M., Hoog, J.C.M. De, Suhr, G., Harvey, J., 2006. Geochemistry of
870 abyssal peridotites (Mid-Atlantic Ridge , 15 ° 20 ' N , ODP Leg 209): Implications for fluid / rock
871 interaction in slow spreading environments. *Chem. Geol.* 234, 179–210.
872 <https://doi.org/10.1016/j.chemgeo.2006.04.011>
- 873 Peach, B.N., Horne, J., Gunn, A.G., Clough, C.T., 1907. The Geological Structure of the North-West
874 Highlands, in: *Memoir of the Geological Survey of Great Britain*.
- 875 Power, M.R., Pirrie, D., Andersen, J.C., Butcher, A.R., 2000. Stratigraphic distribution of platinum-
876 group minerals in the Eastern Layered Series, Rum, Scotland. *Miner. Depos.* 35, 762–775.
877 <https://doi.org/10.1007/s001260050278>
- 878 Rollinson, H., 2007. Recognising early Archaean mantle : a reappraisal. *Contrib. to Mineral. Petrol.*
879 154, 241–252. <https://doi.org/10.1007/s00410-007-0191-y>
- 880 Rollinson, H., Gravestock, P., 2012. The trace element geochemistry of clinopyroxenes from
881 pyroxenites in the Lewisian of NW Scotland: Insights into light rare earth element mobility
882 during granulite facies metamorphism. *Contrib. to Mineral. Petrol.* 163, 319–335.
883 <https://doi.org/10.1007/s00410-011-0674-8>
- 884 Rollinson, H.R., Windley, B.F., 1980. An archaean granulite-grade tonalite-trondhjemitic-granite suite
885 from Scourie, NW Scotland: Geochemistry and origin. *Contrib. to Mineral. Petrol.* 72, 265–281.
886 <https://doi.org/10.1007/BF00376145>

887 Sheraton, J.W., Skinner, A.C., Tarney, J., 1973. The geochemistry of the Scourian gneisses of the
888 Assynt district, in: *The Early Precambrian Rocks of Scotland and Related Rocks of Greenland*.
889 University of Keele, pp. 13–30.

890 Sills, J.D., 1981. *Geochemical studies of the Lewisian Complex of the western Assynt region, NW*
891 *Scotland*. University of Leicester.

892 Smithies, R.H., Ivanic, T.J., Lowrey, J.R., Morris, P.A., Barnes, S.J., Wyche, S., Lu, Y., 2018. Two distinct
893 origins for Archean greenstone belts. *Earth Planet. Sci. Lett.* 487, 106–116.

894 Sutton, J., Watson, J.V., 1951. The pre-Torridonian metamorphic history of the Loch Torridon and
895 Scourie areas in the northwest Highland, and its bearing on the chronological classification of
896 the Lewisian. *Q. J. Geol. Soc.* 106, 241–307.

897 Szilas, K., Kelemen, P.B., Bernstein, S., 2015. Peridotite enclaves hosted by Mesoarchaeon TTG-suite
898 orthogneisses in the Fiskefjord region of southern West Greenland. *GeoResJ* 7, 22–34.
899 <https://doi.org/10.1016/j.grj.2015.03.003>

900 Szilas, K., van Hinsberg, V., McDonald, I., Næraa, T., Rollinson, H., Adetunji, J., Bird, D., Hinsberg, V.
901 Van, McDonald, I., Næraa, T., Rollinson, H., Adetunji, J., Bird, D., 2018. Highly refractory
902 Archean peridotite cumulates: Petrology and geochemistry of the Seqi Ultramafic Complex,
903 SW Greenland. *Geosci. Front.* 9, 689–714. <https://doi.org/10.1016/j.gsf.2017.05.003>

904 Taylor, R.J.M., Johnson, T.E., Clark, C., Harrison, R.J., 2020. Persistence of melt-bearing Archean
905 lower crust for > 200 m.y.— An example from the Lewisian Complex , northwest Scotland.
906 *Geology* 48. <https://doi.org/10.1130/G46834.1/4906652/g46834.pdf>

907 Van Kranendonk, M.J., Collins, W.J., Hickman, A., Pawley, M.J., 2004. Critical tests of vertical vs.
908 horizontal tectonic models for the Archean East Pilbara Granite-Greenstone Terrane, Pilbara
909 Craton, Western Australia. *Precambrian Res.* 131, 173–211.
910 <https://doi.org/10.1016/j.precamres.2003.12.015>

- 911 Weaver, B.L., Tarney, J., 1981. The Scourie Dyke Suite: petrogenesis and geochemical nature of the
912 Proterozoic sub-continental mantle. *Contrib. to Mineral. Petrol.* 78, 175–188.
- 913 Wheeler, J., Park, R.G., Rollinson, H.R., Beach, A., 2010. The Lewisian Complex: insights into deep
914 crustal evolution. *Geol. Soc. London, Spec. Publ.* 335, 51–79. <https://doi.org/10.1144/SP335.4>
- 915 Whitehouse, M.J., Fedo, C.M., 2003. Deformation features and critical field relationships of early
916 Archaean rocks , Akilia , southwest Greenland. *Precambrian Res.* 126, 259–271.
917 [https://doi.org/10.1016/S0301-9268\(03\)00098-6](https://doi.org/10.1016/S0301-9268(03)00098-6)
- 918 Whitehouse, M.J., Kemp, A.I.S., 2010. On the difficulty of assigning crustal residence, magmatic
919 protolith and metamorphic ages to Lewisian granulites: constraints from combined in situ U-Pb
920 and Lu-Hf isotopes. *Geol. Soc. London, Spec. Publ.* 335, 81–101.
921 <https://doi.org/10.1144/SP335.5>
- 922